RSC Advances

ROYAL SOCIETY OF CHEMISTRY

www.rsc.org/advances

Title : Polyorthotoluidine Dispersed Castor Oil Polyurethane Anticorrosive Nanocomposite Coatings

Authors

Mohammad Kashif[1],
[1]Materials Research Laboratory,
Department of Chemistry,
Jamia Millia Islamia,
New Delhi-110025,India
Email: kashif_jmi25@yahoo.co.in

Corresponding Author

Sharif Ahmad[1]
[1]Materials Research Laboratory,
Department of Chemistry,
Jamia Millia Islamia,
New Delhi-110025,India
Fax: (+91-112-684-0229),]
Tel: 011-26981717 ext:3268
Email: sharifahmad_jmi@yahoo.co.in

ABSTRACT

Present article reports the synthesis and corrosion protection performance of polyorthotoluidine (POT) nanoparticles dispersed castor oil polyurethane (COPU) nanocomposite coatings in acid and saline environment. The structure of POT/COPU was confirmed by FTIR and UV-Visible spectroscopic techniques. The nano structure of virgin POT nano particles and in composite was characterized by X-ray diffraction (XRD) and transmission electron microscopy (TEM). The physico-mechanical properties were analyzed using standard methods. The corrosion protective performance was evaluated by weight loss, potentiodynamic polarization and electrochemical impedance spectroscopy in acid medium. While in case of saline environment the corrosion protective performance was investigated in salt mist chamber using 5%NaCl solution for 30 days. The morphological behavior of the corroded and un-corroded coated specimen was investigated by SEM studies. The stipulated acid and saline corrosion mechanism was also discussed.

Keywords: Mild Steel; Polarization; SEM; EIS; Acid corrosion; Kinetic parameters

1. Introduction

For the last few years a growing interest has been developed in the application of conducting polymers and their nano structures, because of their promising physico-mechanical, conducting magnetic, electrochromic and corrosion inhibition properties.[1-7] The nano- conducting polymers due to high surface volume ratio and unique morphology exhibit easy and improved dispersion behavior in non conducting polymer matrix.[8, 9] Hence, these polymers find wide applications in the field of microelectronics, electroluminescent, electrochromic devices, sensors, corrosion inhibitors and coatings.[10-15]The nano-conducting polymers have been dispersed in various polymer matrices like polyester, epoxy, polyurethane etc are used as corrosion protective composite coating materials.[16-18] Among various conducting polymers, polypyrrole (PPy) and polyaniline (PANI) are considered to be the most promising one used for corrosion protection.[13-15, 19, 20] Wang *et al.*[21] has developed PANI dispersed epoxy-polyamide coatings on mild steel. S. Chaudhari and Patil *et al.*[22] reported Poly-orthotoluidiene (POT)-CdO nanocomposite coating for MS. Advincula *et al.*[23] synthesized cross-linked poly(vinylcarbazole) (PVK)-conjugated polymer network (CPN) using electro-polymerization technique on ITO glass. An investigation has been made on the corrosion protective performance of W doped PANI-vinyl coatings on mild steel by S. Sathiyanarayanan *et al*.[13] However, major drawbacks associated with the conducting polymer coatings are their solubility and processing.[24] In order to improve these properties different derivatives of PANI like N,N-Dimethyl aniline, o-and m- toluidine have been used and their modifications with metal, metalloids as well as their copolymers and IPNs with other conducting polymers has been reported.[13-16,24]

Most of the conducting polymer based composite coatings are formulated with the help of synthetic non conducting polymers, which are derived from petrochemical resources involving the use of organic solvents, which produce volatile organic component (VOC). The VOC

produces prominent health hazards and harmful effect to the society and environment. Thus in order to overcome the problem of VOC and to meet the requirements of various environmental acts implemented in this regard. The usage of some alternatives coating materials have been proposed and developed via high solid coating materials, U.V curable, waterborne and low molecular weight vegetable oil based polymeric coatings.[25-30] In context to these VOC free materials, vegetable oils may act as a potential alternative. The vegetable oils like linseed, pongamia, jatropa, soya, castor etc. have been employed for the synthesis of different types of polymeric coating materials like oil based epoxy, alkyd, polyesteramide, PU etc.[31-34] Among these coating materials PUs exhibit promising physico-mechanical and corrosion resistant properties that provide PUs coatings an opportunity to be utilized in automobile industry. However, there is still scope of research for the development of high performance oil based PU coating materials, which may find application in various advance industries like medical, construction, marine, appliances etc.[18]

Considering the promising corrosion protective performance of conducting polymers, here we report the synthesis and formulation of nanostructured POT; a derivative of PANI, dispersed castor oil polyurethane (COPU) nanocomposite coatings on mild steel, their physico-mechanical characterization and corrosion protective performance**.** The corrosion resistance measurements were carried out by weight loss measurements; potentiodynamic polarization, electrochemical impedance and salt spray tests. These studies revealed that the nano-composite coatings exhibit superior corrosion protective performance as compared to those of other reported such coatings.[35-37]

2. Experimental

Materials

Castor oil ($C_{57}H_{104}O_9$, hydroxyl number: 159 mg KOH/g, Mol. wt.:932 g/mol), ethyl methyl ketone, Mol.wt:72.11 g/mol), methanol and ammonium per sulphate (Mol wt. 228.18 g/mol) Merck, India. 2, 4-toluylene diisocyanate (TDI) (Mol wt. 174.06 g/mol; Merck, Germany), were used as received. *Ortho* toluidine monomer (Sigma, Aldrich, USA) was double distilled prior to use**.**

Synthesis of Nano Polyorthotoluidine (POT)

POT nanoparticles were synthesized as per our earlier reported method.[38] *o*-toluidine monomer (0.1 M) was dissolved in methyl alcohol (50 ml) at room temperature (30 ^{o}C). The oxidant solution was prepared by dissolving APS (10 g) in aqueous HCl solution (100 ml, 1 M). Both solutions were precooled to 0–5 ^{o}C in an ice bath. The monomer solution was placed in a round bottom flask and inserted in an ice bath on a magnetic stirrer. An APS solution was then added to the *o*-toluidine solution dropwise over a period of 30 min with constant stirring. The mixture was stirred in the ice bath for 5 h to ensure complete mixing. A dark green precipitate of POT was obtained, which was filtered, repeatedly washed with distilled water to remove the excess of acid and impurities and dried under vacuum at 80 ^{o}C for 72 h. The TEM studies confirmed the nano size of POT particles.

Synthesis of castor oil polyurethane [COPU]

Castor oil polyurethane was prepared by reported method.[39] Castor oil was reacted with TDI (NCO/OH ratio1:2) in a three-necked round bottom flask under nitrogen gas purge. The reaction was carried out at room temperature (30 ^{o}C) with continuous stirring for 2 h. The polymer of COPU was isolated as a viscous liquid.

Preparation of Poly (*o*-toluidine) (POT) nanoparticles dispersed castor oil-polyurethane nanocomposite (POT/COPU)

The POT/COPU nanocomposites were formulated by mixing the different amount of POT (0.25 wt%, 0.5 wt%, 1.0 wt%) in 10 wt% solution of COPU in ethyl methyl ketone. The POT was found to be homogeneously dispersed in COPU up to 1.0 wt%, beyond which, the POT was fail to disperse in COPU solution, which can be attributed to the low volume and higher surface area ratio of the POT nanoparticles, hence, the loading of POT beyond 1.0 wt% was not attempted. The POT dispersed COPU mixture was continuously stirred for a period of 4-5 hours at room temperature (30 ^{o}C) to ensure the uniform and stable dispersion of POT in COPU. The constituent mixture was then placed in a rotary evaporator to remove the solvent. The reaction scheme for the same is given in Fig. 1. The formation of the POT/COPU nanocomposites was confirmed by FT-IR, UV-visible spectroscopy and TEM analysis.

Characterization:

Spectral Analysis

FTIR spectra of the polymer nanocomposite (POT/COPU) was determined on a PerkinElmer 1750 FTIR spectrophotometer (Perkin Elmer Instruments, Norwalk, CT) with the help of NaCl cell. UV-visible spectra were taken on Perkin-Elmer-LAMDA-ez-221 in solution form.

Thermal Analysis

Thermo-gravimetric analysis (TGA) of POT and POT/COPU was performed using the SII EXSTAR 6000 analyzer (Japan) from 40 ^{o}C to 800 ^{o}C in nitrogen atmosphere at the rate of 20^{o}C/min.

Size and Morphological analysis

X-ray diffractograms were recorded on Philips X-ray diffractometer model Philips W3710 using copper Kα radiation. Transmission electron micrographs (TEM) were taken on Morgagni 268-D TEM, FEI, USA. The samples were prepared by placing an aqueous drop of POT and POT/COPU on carbon-coated copper grid, subsequently drying in air before transferring it to the microscope operated at an accelerated voltage of 120 Kv.

Physico-mechanical Characterization

The specific gravity and refractive index of COPU and POT/COPU nano-composite coating materials were determined using ASTM D792 and ASTM D542 methods respectively. The specular gloss at 60^{o} (gloss meter, model RSPT-20; digital instrument Santa Barbara CA), scratch hardness (BS 3900), and impact resistance (IS: 101 par 5/sec-31988) were determined on COPU and POT/COPU coated 70 x 30 x 1 mm size mild steel strips. The five coated samples were tested and their mean average values were determined using error bars representing standard deviation.

Electrical Conductivity Measurements

The conductivity of POT/COPU films was measured by standard four probe method using Keithley DMM 2001 and EG&G Princeton Applied Research potentiostat model 362 as current source. For each composite, three specimens were taken and their mean average was reported.

Coating preparation on mild steel

The 70 wt% solution of COPU and POT/COPU naocomposites (using different weight percentage of POT (i.e., 0.25POT/COPU, 0.5 POT/COPU and 1.0POT/COPU, where prefix indicate the percentage of POT) in ethyl methyl ketone, were applied by brush technique, on finely polished and degreased mild steel strip (IS : 6240 HR: Carbon 0.16%, Manganese 0.30%,

Silicon 0.25%, Sulphur 0.030%, Phosphorous 0.030%, Aluminium 0.02%, Fe 98.0%) of 70 mm x 30 mm x1 mm and 25 mm x 25 mm x 1 mm sizes used for physico-mechanical and corrosion resistant tests respectively. The coating thickness of COPU and POT/COPU were found in the range of 102-106 µm.

Corrosion resistance measurements

Corrosion rate analysis by weight loss method

Corrosion resistance performance of COPU and POT/COPU coated MS with reference to uncoated MS were investigated in acid (3.5 wt% HCl**)** environment using ASTM G31 method. The rough edges and faces of the uncoated specimen have been grounded to 120-grit finish on water cooled polishing unit and marked for identification with vibratory tool. After washing with 10% nitric acid for 10 minutes at 50 °C, the sample was lightly scrubbed with slurry of Alconox cleaner using soft bristle brush. Further, the finely finished samples were rinsed with distilled water, methanol, acetone, and then dried. The length, width, and thickness of dried samples were accurately measured. The test was performed by weighing samples before and after the immersion exposure in corrosion flasks. Each flask was equipped with an Allihn condenser to prevent evaporation. Test samples were suspended using fluoropolymer filament within the flasks in such a way that they did not touch either the side wall of the vessel or each other. The total surface area of the test sample per flask was controlled so that the minimum recommended solution volume to surface area ratio (0.2 ml/mm^2) was maintained. The flasks were kept in the static condition without agitation or aeration. The corrosion cells were visually monitored periodically during the immersion time.

The protective behavior of the coatings against the dissolution of MS was evaluated by calculating the corrosion protection rate (CR) for each one of the samples. The calculation was performed using the following expression.[39]

$$CR = \frac{\Delta g}{Atd}$$

Where Δg is the change in weight loss of the specimen, A is the area of the specimen, t is the time (year), and d is the density of the specimen. The results were given in milli-inches per year (MPY).

Potentiodynamic and Electrochemical impedance spectroscopy (EIS) measurement

Corrosion resistance performance of COPU and POT/COPU coated as well as uncoated MS strips were evaluated by potentiodynamic and electrochemical impedance spectroscopy (EIS) measurements in HCl (3.5 wt%) at room temperature (25 ^{o}C) using micro Autolab type III with FRA unit (μ3AVT 70762, Netherlands) potentiostat for the period of 20 days. The Tafel polarization curves in 3.5 wt% HCl were obtained using a three-electrode electrochemical cell (EG&G Flat cell) containing platinum gauze as counter electrode, Ag/AgCl as reference electrode and test specimen (coated and uncoated mild steel specimen) as working electrodes. The test specimens were fitted in electrochemical cell with 1cm^2 area of the sample exposed to the corrosive media. The potentiodynamic tests were performed in the potential range of -0.4 V to 1.4 V at a sweep rate of 0.5mVs^{-1}.

The potentiodynamic studies were made after exposing the specimen in electrolyte for 30 min. The percent inhibition efficiency IE (%) was calculated, using following equation.[40]

$$IE\% = \frac{I'corr - Icorr}{I'corr} \times 100$$

Impedance measurements were carried out at a frequency range of 100 KHz to 0.1 Hz with an AC amplitude of 10mV after 30 minutes of immersion in the said corrosive environment up to 20 days.

3. Results and Discussion

Spectroscopic Analysis

FT-IR spectra of POT and POT/COPU

The FTIR spectra of POT/COPU (Fig. 2) nanocomposite showed a significant negative shift of -15 and -16 cm^{-1} in –NH and –NHCO stretching bands respectively, i.e. from 3356cm^{-1} of pristine POT to 3341cm^{-1} for –NH stretching and –NHCO peak from 1744 cm^{-1} to 1728 cm^{-1}.[39] The negative shift in –NH and urethane of POT/COPU indicate that the urethane group of the COPU interacts strongly with that of –NH group of the POT.[39] The broadness of the NH peak attributed to the presence of strong hydrogen bonding in between –NH and–NHCO groups. The carbonyl of POT/COPU absorption peaks in the nanocomposites of POT/COPU observed at 1728 cm^{-1} and 1650 cm^{-1} exhibit a shift of -16 and -15 cm^{-1} as compared to that of pristine COPU, which can be further correlated to the intense hydrogen bonding between –NH of POT and –NHCO of COPU (Fig.1). The peak at 2253 can be attributed to CN stretching vibration.

UV-Visible spectroscopy

The UV-Visible spectra of POT and POT/COPU are given in Fig. 3. The absorption peak at 330 nm can be correlated to the π-π* transition of benzene ring, which was related to the extent of conjugation of adjacent phenylene rings in the polymer chain and the charge transfer from valence band to conduction band.[45] The absorption peak in the visible region (550-700 nm), showed the excitation of the imine units present in the backbone of POT, induced donor-acceptor interactions between benzenoid-quinonoid rings leading to n-π* transitions.[41] The broad

absorption peak around 650-700 nm observed in pristine POT can be correlated to the presence of highly delocalized electrons. The spectra of POT/COPU composites showed a blue shift of 100 nm in the polaronic transition peak, which was observed at 600 nm. The increase in the intensity of the polaronic transition peaks upon higher loading of POT in COPU and the increase in shifting of the polaronic transition peaks confirmed the restriction in the delocalization of polarons induce in the POT chains, this can be attributed to the electrostatic interaction between the carbonyl group of COPU and the amide of POT. The physical interaction of POT chains with COPU segments hinders the path for the charge conduction, causing a significant decrease in the conductivity of the POT from 5.01×10^{-3} S/cm to 5.7×10^{-4}S/cm.

TEM Analysis

The TEM micrograph of 1.0-POT/COPU, Fig. 4, exhibited chain like dispersion of POT particles of average size 20-30 nm led to the formation of two phase system. The dark particles correspond to the POT nanoparticles while the bright phase can be correlated to COPU matrix (Fig. 4). The POT nanoparticles within the COPU matrix appear to be globular and highly agglomerated upon increasing (more than 1.5%) the loading of POT.

X-Ray Diffraction Analysis

The X-ray diffractogram of COPU was reported in our earlier paper,[39] where as in case of POT (Fig. 5 a) a pronounced peak was observed at 20 A^{o}, corresponding to a full width at half maxima (FWHM) of 2.5, having an average particle size of 20 nm, calculated by Scherer equation.[42] This peak confirm the semicrystalline behavior of POT. The significant impact of nanostructured POT has been observed on the amorphous nature of COPU matrix (Fig. 5 b). The diffraction pattern in the POT/COPU nanocomposite showed the presence of a prominent peak (a hump) at 25 A^{o} . The peak exhibited a positive blue shift of 5 A^{o}, can be corroborated to the encapsulation of POT

within the amorphous COPU matrix. The encapsulation also led to a reasonable decrease in the peak of POT.[46, 47] This peak further confirms the dispersion of POT nanoparticles in coating.

Thermal Analysis:

Thermograms of POT, COPU and POT/COPU nanocomposites revealed that the dispersion of POT in the COPU matrix increased the thermal stability (Fig. 6) . Thermograms of POT, COPU and POT/COPU nanocomposite showed similar decomposition pattern (Fig. 6). The 10 wt% decomposition of pristine COPU was found at 115 ^{o}C and 20 wt% at 205 ^{o}C while 50 wt% decomposition was observed at 325 ^{o}C. The pristine POT exhibits 10 wt%, 20 wt% and 50 wt% decompositions at 228 ^{o}C, 320 ^{o}C and 500 ^{o}C, respectively. For various compositions of POT/COPU nanocomposite, the thermal decomposition temperatures for 10 wt%, 20 wt% and 50 wt% was found to be higher than that of pristine COPU but lower than that of pristine POT (Fig. 6). It was further observed that the thermal stability of nanocomposites was increased with increase loading of POT in COPU. The thermal stability study revealed the following trend: pristine POT>1-POT/COPU>0.5-POT/COPU>0.25-POT/COPU>COPU. The increase in the thermal stability of composites can be correlated to the hydrogen bonding between C=O of COPU and NH of POT (FTIR spectra Fig. 2) and loading of POT in COPU.

Physico-mechanical Characterization

The values of physico-mechanical properties for COPU and POT/COPU nanocomposites coatings (Table-1) revealed that the specific gravity of POT/ COPU nanocomposites increases with the increased loading of POT in COPU. The linear decrease in refractive index and gloss values were observed with the increased concentration of POT in nanocomposite (Table-1) can be correlated to the opaque nature of conducting polymer POT.[39]

The nanocomposite coatings showed the decrease in dry to touch and dry to hard times than that of COPU coatings. However, with the increase in the loading of POT in COPU the dry to touch and dry to hard time was increased (Table-1). The scratch hardness value of COPU coating was found to be 1 kg, while that of POT/COPU (0.25% to 1.0% POT) nanocomposite coatings was found much higher (from 7.5 kg, to 8.2 kg). The increase in scratch hardness values of nanocomposites can be attributed to the synergistic effect of the POT/COPU nanocomposite, the presence of POT (conducting polymer) induced stiffness in nanocomposite coatings, further enhanced the mechanical properties of these coatings. The impact resistance values in case of POT/COPU nanocomposite coatings (from 150 to 200 lbs/inch) were found higher than that of COPU coatings (100 lbs/inch). As a characteristic of oil based polymeric coatings, all these coatings passed the 1/8" conical mandrel bend test.[39] The physico-mechanical properties of POT/COPU were found much higher than the other reported POT based coatings.[41, 43]

Conductivity measurement

Conductivity measurements were carried out at room temperature (30 ºC). The values for conductivity of POT (Fig. 7) was found to be 5.01×10^{-3} S/cm, while upon loading the 0.25 wt% of POT in COPU, the conductivity decreased by an order of magnitude (5.96×10^{-4} S/cm). Further on increasing the loading of POT from 0.25 to 1.0 wt%, a slight increase in conductivity was observed (6.23×10^{-4} S/cm for 0.5-POT/COPU and 6.89×10^{-4} S/cm for 1.0POT/COPU). The conductivity data have not exhibited any well defined percolation threshold. Since, the transition from the insulating state of the COPU matrix to the conducting state of the nanocomposites was observed at ~0.5 wt% loading, it can be concluded that the percolation limit may fall below 1.0 wt% loading of POT.

Corrosion resistant measurement

Corrosion rate analysis using weight loss measurement

The corrosion resistance performance of COPU and POT/COPU coated and uncoated mild steel strips (Fig. 8) were investigated for a period of 480 h in 3.5wt% HCl solution. After 480 h of immersion, the coatings of POT/COPU showed no visual deterioration or dissolution. The uncoated MS showed the dissolution of metal in HCl with corrosion rate of 3.0×10^{-1} mpy. The pristine COPU coatings started deterioration after 48 h and were completely peel out within 96 h, which revealed a rapid deterioration with corrosion rate of 9.0×10^{-2} mpy. However, the corrosion rates for 0.25, 0.5 and 1.0 POT/COPU nanocomposite coated MS were found to be 5.2×10^{-3}, 4.2×10^{-3} and 3.7×10^{-3} mpy respectively. The high corrosion resistance performance of 1.0POT/COPU nanocomposites coatings in HCl medium can be attributed to the intimate and homogeneous dispersion of POT, which acted as an efficient barrier.[22] The presence of POT further provided resistance to the permeability of corrosive ions at the coating-metal interface. The interaction between NH of POT and C=O of COPU led to the formation of highly compact and well adhered coatings of POT/COPU nanocomposites, which has effectively induced protection to the metallic surface. Mobin et al. had find out that Poly (aniline-co-o-toluidine) and Poly (pyrrole-co-o-toluidine) coated steel under 0.1 M HCl shows corrosion rate of 5.02 and 4.11 mpy, which is much higher than the POT/COPU coatings.[37] 2.0-PANI/COPU coatings in HCl shows corrosion rate of 0.38 mpy, which is also much higher than that of 1.0-POT/COPU (3.7×10^{-3} mpy). This further confirmed that the interaction of POT with COPU make a strong adherence on mild steel which induces far superior corrosion resistance properties in POT/COPU coatings.

Potentiodynamic polarization measurement

The corrosion protective performance of COPU and POT/COPU nanocomposite coated and uncoated MS was further evaluated using potentiodynamic polarization technique in 3.5 wt%

HCl at different interval of times (Fig. 9). The values for corrosion potential (E_{corr}), corrosion current density (I_{corr}), beta cathodic (βc), beta anodic (βa) and inhibition efficiency (%IE) of COPU and POT/COPU nanocomposite coatings were obtained from their potentiodynamic polarization curves (Table-2). The E_{corr} for COPU (-1.091 V) coated MS showed a positive shift as compared to that of bare MS (-1.173 V). The positive shift in E_{corr} confirmed that the COPU coatings led to the decrease in the anodic current of the corrosion reaction and offered resistance to MS against corrosion.[43] The POT/COPU nanocomposite coatings showed further increase in their E_{corr} values with the increased loading of POT in COPU (-0.902, -0.812 and -0.738 V for 0.25POT/COPU, 0.5POT/COPU and 1.0POT/COPU coatings respectively). The I_{corr} of COPU coated MS was found to be lower than that of uncoated MS, which further decreased with the increased loading of POT (Table-2). This observation from above trend suggested that coated MS control both cathodic and anodic reaction and thus provide protection to the MS substrate and the protection provided by POT/COPU coating was more than that of COPU coating. Among different compositions of POT/COPU coatings 1.0POT/COPU showed best corrosion resistant properties as exhibited by its highest value of E_{corr} (−0.738 V) and lowest value of I_{corr} (8.30×10^{-8} A/cm^2) after 0.5h. The inhibition efficiency of 1.0POT/COPU was 99.0% which was found to be higher than those of 0.25POT/COPU and 0.5POT/COPU coated MS (97% and 98%) respectively. The higher corrosion resistant performance of POT/COPU coating as compare to COPU coating can be correlated to the fact that conducting polymer act as a barrier, which decrease the amount of water, oxygen, and corrosive ions to reach at the metal−coating interface and form protective passive layer on the stainless steel surface because of its redox catalytic properties.[44] Conducting polymer act as hydrophobic material, which also induces protection to the metal through the reflection of wet corrosive species.[44] Therefore, as the amount of POT in

COPU increases its corrosion resistant properties was also increased. It was further observed that as the exposure time increases a drop in E_{corr} (Table-2), and increase in I_{corr} for both COPU and POT/COPU coated MS was observed (Table-2). This observation suggested that coating began to deteriorate on prolonged immersion. The COPU coating completely spelled out after 240 h, however, POT/COPU coating provide protection to the MS up to 480 h, although their protective efficiency decreased from 99% to 84% for 1.0POT/COPU. This can be attributed to the fact that with prolonged immersion corrosive ions accumulated at the coating-metal interface, causing the deterioration of coatings. Hence, the potentiodynamic studies revealed that the corrosion protective performance of these coatings was found to increase with the increased loading of POT in COPU, The highest corrosion protective performance was recorded in case of 1.0POT/COPU nanocomposite coating (Table-2).

The corrosion protective performance of POT/COPU coating is remarkably higher than those reported by Mobin et al,[37] who found that the Poly (aniline-co-*o*-toluidine) and Poly (pyrrole-co-*o*-toluidine) coated steel after one month of immersion in 0.1M HCl shows inhibition efficiency only up to 78.41 and 78.45 mpy respectively, which was much lower than that of 1.0-POT/COPU (99.76%) . No other work had been reported on corrosion resistance performance of POT in HCl by potentiodynamic polarization studies. However, Patil et al[36] have electro polymerized POT on steel and find out that in 3.0% NaCl, the E_{corr} and I_{corr} values were 0.089 V and 5.11×10^{-8} A/cm^2 respectively, which was slightly lower than that of POT/COPU coating (I_{corr}= 7.19×10^{-8} A/cm^2).

Electrochemical Impedance Spectroscopy (EIS) Measurement

Electrochemical impedance spectroscopy (EIS) was employed to investigate the corrosion characteristics of the uncoated, COPU and POT/COPU coated MS specimen, the Nyquist and

bode plots for these systems are given in Figs. 11-13, respectively. Based on the impedance plots, an appropriate equivalent circuit was proposed (Fig. 14). The equivalent circuit consists of two resistance parameters; polarization resistance (R_p), pore resistance (R_{pore}), two capacitances; one component (C_{cl}) in series with R_{por}, corresponding to one of the three resistance of the outer layer of coatings, and C_{dl} is the inner layer/interface capacitance of the coating. The circuit elements calculated from the fitting results of the COPU and POT/COPU coatings are given in Table-3-6. The impedance values were reproducible ±2–3%. FRA Software was used for plotting, graphing and fitting the data.

Kinetic Parameters

(a) Polarisation resistance (R_p)

The R_p value of COPU after 24 h was found 5.6 × 10^5 Ωcm^2, which was found to decrease with the increased immersion time and reaches to 6.7 × 10^2 Ωcm^2 after 240 h. Such a low value of R_p indicated that the COPU coating was deteriorated after this period of time. However, the R_p value for POT/COPU coatings was found much higher than that of COPU (Table-4-6), which further increased with the increase in loading of POT in COPU from 0.25 to 1.0 wt%. (Table-4-6). Furthermore, as the immersion time increases the R_p value were found to decrease sluggishly (Table-4-6). The 0.25-POT/COPU nanocomposite coating has higher initial polarization resistance (R_p> 10^7Ωcm^2) but after 24 h it was begun to drop with time and reached to a value of 10^5 Ωcm^2 after 480 h, below which corrosion protection ability of the coating seemed to be lost.[45] 1.0POT/COPU coatings has very high R_p value 3.0 ×10^{10} Ωcm^2 (24 h) and drop to 5.2 ×10^7 Ωcm^2 (480 h), such a high value of R_p even after 480 h of exposure to corrosive media shows that the 1.0POT/COPU coating composition provide maximum protection to the MS.

Nyquist and Bode plots of COPU and POT/COPU nanocomposite coated MS exposed to 3.5 wt% HCl solution for periods of 24, 240 and 480 h are shown in Fig. 11-13. With the increased immersion time, the decrease in the diameter of the Nyquist plot was recorded (Fig. 11-14) this can be attributed to the decrease in R_p value.

The Bode plot in Fig. 11 shows the impedance value of the COPU coated MS, which showed that the impedance value decreased sharply from 10^5 to 10^4 ohm after 120 h of exposure and reached to 10^2 ohm after 240 h in lower frequency range. In the medium frequency zone, a linear relationship between log |Z| vs log f with a slope of 1.3 (value of log f) has been observed after 24 h and was found to increase up to 1.8 after 240 h exposure. In higher frequency region impedance value decreased in the manner of 10^4, 10^3 and 10^2 ohm (100 Hz frequency) after 24, 120 and 240 h respectively. These values thus represent the failure of COPU coating, i.e., the point at which a coating no longer provided corrosion protection. For POT/COPU coated MS initially (after 24 h) the impedance was found in the range of 10^{10}-10^7 ohm in lower frequency region, which was further dropped to 10^7-10^5 ohm on longer exposure, remarkably higher than that of COPU coated MS. In higher frequency region (100 Hz) also the impedance value of 0.25POT/COPU coated MS was found in the range of 10^6 to 10^5 ohm, which was much higher than that of COPU, coated MS. The higher impedance value of POT/COPU coated MS in lower as well as in higher frequency region would imply that these coating systems provided protection to the metal substrate. The higher impedance values depicted by the Bode and Nyquist plots for 0.5POT/COPU and 1.0POT/COPU nanocomposite coatings (Figs. 12, 13) for all immersion periods suggested that these coatings provided superior protection against acid corrosion (Table-4-6).

(b) Pore resistance (R_{pore})

The initial R_{pore} value at low frequency range for COPU was found 4.1×10^5 Ωcm^2, which decreases with the increase in immersion time and reaches to 5.8×10^2 Ωcm^2 (after 240 h), which was reasonably low. Such a low value for R_{pore} suggested that the electrolyte start to penetrate through the coating at the interface that leads to the deterioration of MS.[48]

For POT/COPU coatings the R_{pore} value increases with the increased loading of POT. The R_{pore} value after 24 h for 0.25POT/COPU, 0.5POT/COPU and 1.0POT/COPU coatings was found 2.5×10^7, 2.0×10^9 and 2.8×10^{10} Ωcm^2 respectively. This increase in R_{pore} can be attributed to the fact that with the increased loading of conducting polymer the sealing of pores in coating occurs,[22] which enhances the pore resistance property of POT/COPU coating. It was further observed that with time the R_{pore} value decreases for all the compositions of POT/COPU coatings, i.e. after 480 h the R_{pore} value for 0.25POT/COPU, 0.5POT/COPU and 1.0POT/COPU was found 2.6×10^4, 5.6×10^5 and 4.6×10^7 Ωcm^2 respectively. The decrease in pore resistance with respect to the immersion period (Table-6) for all the compositions indicated that pores were open and leading to the penetration of electrolyte.[49] However, R_{pore} value for 1.0POT/COPU coatings have highest value both after 24 h and 480 h among all the compositions. This suggested that this composition of coating provide maximum protection to the MS.

(c) Coating capacitance (C_c)

The capacitance of a coating is used to measure the quantity of water absorbed at the coating-metal interface. Generally, in aqueous environment, coating capacitance (C_c) increases at the initial stage of exposure then after an incubation period it become constant. The EIS experiments showed that the COPU coatings have higher C_c values (6.4×10^{-7} and 8.2×10^{-5} F/cm^2 after 24 and 240 h respectively) as compared to those of all the compositions of POT/COPU coatings, this can be correlated to the fact that the electrolyte easily penetrate through the pores present in

COPU coatings, while in case of POT/COPU nanocomposites the presence of POT induces locking effect, which did not allow electrolyte to penetrate at the coating-metal interface.[55] The POT/COPU coatings show an increase in C_c values with the increased exposure time (Tables-4–6), since with the prolonged immersion time the electrolyte penetrate at the coating metal interface.[49, 50]

(d) Double layer coating capacitance (C_{dl})

The double layer capacitance is associated with an area exposed to the electrolyte (i.e. the delaminated area). Its formation occurs after the penetration of an electrolyte through the coating to the substrate.[49] The formation of corrosion product at coating-metal interface on the penetration of electrolytes inside the coatings, which reduces the area of double layer capacitor, causing an increase in C_{dl} value. The stable value for C_{dl} of coating was an indication for the formation of stable interface.[51] The presence of corrosion products at the metal-coating interface allowed to absorb more electrolytes through the coating, which led to an increase in the dielectric constant of the coating and can be attributed to the deterioration of coating with longer immersion time. The higher C_{dl} values (7.8×10^{-7} F/cm^2) for COPU coating even after 24 h of exposure suggested that the electrolyte easily penetrates and reaches to the coating-metal interface in the acidic environment. The 1.0POT/COPU coating exhibits lowest C_{dl} value (4.1×10^{-10} and 5.7×10^{-8} F/cm^2 after 24 and 480 h respectively) among all compositions of POT/COPU coatings. This confirmed that the 1.0POT/COPU coatings have highest stable coating/metal interface.[52]

EIS also reveal that the corrosion resistant performance of POT/COPU is remarkably higher than that of other reported such systems. Patil *et al*[22,53] has developed POT/CdO and POT/ZrO_2 nanocomposite coatings on mild steel and find out that the R_p value 6.23×10^3 Ω and 1.6×10^3 Ω

respectively. H. Wei *et al*[54] have developed multi-walled carbon nanotube (MWCNT) dispersed polyurethane coating on steel and find out its anticorrosive performance under 3.0wt% NaCl, he observed R_p and R_{ct} value 4.49×10^3 and 6.74×10^4 Ω. Wang *et al*[21] have reported the corrosion resistant performance of PANI nanofibre containing Epoxy polyamide coating showing the R_c and R_{ct} value 8.87×10^6 and 2.12×10^6 Ω respectively. These values of kinetic parameters are much lower than that of POT/COPU coating which lies in the range of 10^{10} Ω. However no other work has been reported in HCl environment.

The EIS studies revealed that the corrosion resistance performance of coatings have increased with the increase loading of POT, which act as a filler particle, sealed the pores on the surface of the coatings and protect the MS from corrosion.

Salt spray test

Salt Spray test (SST) on COPU and POT/COPU coating was conducted for a period of 720 h in 5.0 wt% NaCl solution. The uncoated MS specimen was tested as a control. Initially, the coated and uncoated specimen have glossy shiny surface, with the exception of a purple color on the POT/COPU coated specimen. After 48 h of SST the uncoated specimen lost their glossy shiny appearance, further, the entire surface of uncoated MS was covered with dark gray patches, causing significant corrosion damage (Fig. 15e). The COPU coated specimen showed loss in gloss after 144 h, while the POT/COPU nanocomposite coated samples show loss in gloss after 288 h, no damage was observed on the coating surface, even after 720 h (Fig. 15g), on the other hand the COPU coated MS showed some sign of deterioration after 240 h (Fig 15f). The SST clearly revealed that the presence of POT in POT/COPU nanocomposite coatings provide high corrosion protection efficiency in saline medium. The decrease in gloss for COPU and POT/COPU with time can be attributed to the deposition of NaCl crystals at the surface of

coatings, which led to the breaking of the bond of coating material that causes the roughness and deterioration of the surface.

Morphological studies

The surface morphology of uncorroded POT/COPU coated and corroded COPU, POT/COPU coated as well as uncoated MS in HCl environment was investigated by SEM technique. The un-corroded POT/COPU nanocomposite coatings have a uniform and compact surface structure (Fig. 15a). The uniform dispersion of POT nano-particles in the COPU matrix was observed, which led to the formation of homogenous single phase coatings. The dense, uniform and continuous structure of the coating can be correlated to the higher corrosion protective performance of POT/COPU coatings.

The SEM micrograph of acid corroded uncoated MS specimen showed intergranular corrosion along with the formation of cracks and holes, led to the fast dissolution of MS (Fig.15b). The COPU coated MS under HCl after 480 h immersion test showed the formation of pits and holes causing the degradation of coating (Fig 15c). In case of 1.0-POT/COPU coated MS, the presence of POT in COPU made the coating more adherent, the coating was remained undisrupted. However, the agglomerated POT particles along with some coating materials were uniformly precipitated out in the form of particles at the surface of coating, which were remain intact within the coating (Fig. 15d). The corroded uncoated MS specimen in NaCl (Fig 15e) showed the formation of deep cracks and pits leading to the fast dissolution of metal. The deposition of NaCl crystal on the corroded MS surface was also visible, while in case of COPU coated specimen (Fig. 15f) the corrosion products were precipitated out at few places in the form of patches. The 1.0-POT/COPU coating under NaCl environment showed the evidence of slightly low rate of

corrosion, can be attributed to the presence of fine cracks in the coatings the deposition of fine crystals of NaCl on the surface of the coating was also evident (Fig. 15g).

Corrosion protection mechanism

Conducting polymer based coating provides protection through redox and barrier mechanism in different corrosive environment. H. Takenouti *et al*[55], establish the corrosion protection mechanism of conducting polymer based coatings, using PAni and PPy, by measuring the local potential and current, and impedance spectra around the defect area of the coating, found that in tap water the conducting polymer layer is actually able to passivate a defect area. J.Y Lee *et al*[56] investigated the corrosion protection ability of polyaniline (PANI) coating for mild steel corrosion in saline and acid by electrochemical impedance spectroscopy. The impedance behaviour is best explained by a mediated redox reaction in which PANI passivates the metal surface and reoxidizes itself by dissolved oxygen. Patil *et al* [22] proposed barrier mechanism for POT/Cdo nanocomposite coatings in 3.5%NaCl solution. However, the corrosion protection mechanism of conducting polymer dispersed polyurethane coating is yet not reported. The POT/COPU coatings show the formation of a compact iron/dopant complex layer at the metal-coating interface, which act as a passive protective layer till the POT has capability to undergo a continuous charge transfer (reduction reaction) at the metal-coating interface, where the POT is reduced from emeraldine salt form (ES) to an emeraldine base (EB).[49] The polar group present in COPU like carbonyl, amide and –NH group present in POT developed a physical interaction with the Fe^{2+} ions present in the MS. These strong interactions adhered the coating on metal substrate. Furthermore, POT particles act as a nano filler, which seals the pores on coating surface produce locking effect that provide further strength to the coating. In addition to this POT nano-particles introduce roughness at the nano-scale, create air pockets within the COPU

matrix, which induces the hydro-phobicity and reduces the surface wet-ability of the coating, results in the remarkably higher corrosion resistant performance.[57] The presence of $–CH_3$ group in POT provide flexibility and also induces stiffness to the coating material, which was evident from the high scratch hardness value (7.5 to 8.2 Kg) as compared to earlier reported MO-PANI/COPU coatings (2.5-4.0 Kg).[39] However, the accumulation of excessive corrosive ions led, a breakdown of the passive layer resulted in the deterioration of coatings. This type of corrosion protection usually depends on the strength of the passive oxide film and the interaction of –NH of POT, C=O group of COPU with the iron substrate, which allow to impedes the penetration of the corrosive ions.

Conclusion

POT/COPU nanocomposite was prepared by solution blending technique. The minimal dispersion (0.25 wt%-1.0 wt%) of POT in COPU significantly enhances the thermal stability, physico-mechanical properties and corrosion resistance performance of these coatings. Potentiodynamic and EIS measurement further showed that the POT/COPU coated MS effectively provide the protection through barrier mechanism against acid and salt medium to the mild steel. Salt spray test also revealed the similar behavior of coatings to that of acid environment. The POT/COPU coatings have shown far superior corrosion protective performance as compared to that of COPU coatings in acid and saline environment.

Acknowledgement

The author authors are also thankful to the Naval Research Board (NRB) for providing the financial assistance, vide sanction no DNRD/05/4003/155 DATED 03/10/2008.

Dr. Mohammad Kashif is also thankful to CSIR (New Delhi, India) for financial support through Research Associateship [RA] against Grant No. 05/466 (0160)/2K13-EMR-I.

References

1. P. Chandrasekhar, ed. Kluwer, Academic Publishers, Boston, 1999, pp 760.
2. A.G. MacDiarmid, *Chem. Int. Ed.,* 2001, **40**, 2581.
3. N. Hall, *Chem. Commun.,* 2003, **1**, 1.
4. S. Neves, W.A. Gazotti, M.A. De-Paoli, ed. H.S. Nalwa, American Scientific Publishers, Los Angles, 2nd ed.; 2004, Vol. 2, pp. 133–152.
5. R. Gangopadhyay, ed. H.S. Nalwa, American Scientific Publishers, Los Angles, 2nd ed.; 2004, Vol. 2, pp. 105–131
6. A.J. Epstein, ed. R. Farchioni and G. Grosso, Springer, Amsterdam, Vol. 41, 2001, Vol. 41, pp. 3.
7. X. Li, Y. Zhao, T. G. Zhuang and Gu, Q. Wang, *Colloid Surf. A.,* 2007, **295**, 146.
8. H.Zhang, Q. Zhao, S. Zhou, N. Liu, X. Wang, J. Li, and F. Wang, *J. Power Sourc.,* 2011, **196**, 10484.
9. P. Banerjee and B. M. Mandal, *Synth. Met.,* 1995, **74**, 257.
10. X. Lua, W. Zhanga, C. Wanga, T.C. Wenb, and Y. Weic, *Prog. Polym. Sci.,* 2011, **36***,* 671.
11. X. Luo and X. T. Cui, *Acta Biomaterialia,* 2011, **7**, 441.
12. M. C. Kane, R. J. Lascola and E. A. Clark, *Rad. Phys. & Chem.,* 2010, **79**, 1189.
13. K. Kamaraj, V. Karpakam, S. Sathiyanarayanan, S .S. Azim and G. Venkatachari, *Electrochim. Acta,* 2011, **56**, 9262.
14. V. Shinde and P. P. Patil, *Mat. Sci. & Eng. B,* 2010, **168**, 142.
15. B. Zeybeka, N. O. Pekmezc and E. Kilic, *Electrochim. Acta,* 2011, **56**, 9277.
16. S. Jafarzadeh, A. Adhikari, P. Sundall and J. Pan, *Prog. Org. Coat.,* 2011, **70**, 108.
17. A. Mostafaei and F. Nasirpouri, *Prog. Org. Coat.,* 2014**, 77***,* 146.
18. D. K. Chattopadhyay and K. V. S. N. Raju, *Prog. Polym. Sci.,* 2007**, 32**, 352.
19. E. Armelin, R. Pla, F. Liesa, X. Ramis, J. I. Iribarren and C. Alemán*, Corros. Sci.,* 2008, **50**, 721.
20. P. Herrastia, A. N. Kulak, D. V. Bavykinb, C. Ponce de Léonb, J. Zekonytec and F.C. Walsh, *Electrochim. Acta,* 2011, **56**, 1323.
21. H. Zhang, J. Wang, X. Liu, Z. Wang and S. Wang, *Ind. Eng. Chem. Res.,* 2013, **52**, 10172.
22. S. Chaudhari, A. B. Gaikwad, P. P. Patil, *J. Coat. Technol. Res.,* 2010, **7,** 119.
23. F. F. Antonio, N. C. Estillore, T. M. Fulghum and R. C. Advincula, *ACS Appl. Mat. Int.,* 2010**, 2**, 3726.
24. A. F. Baldissera and C. A. Ferreira, *Prog. Org. Coat.,* 2012, **75**, 241.
25. H. Xie, L. Hu, Y. Zhang and W. Shi, *Prog. Org. Coat.,* 2011, **72**, 572.
26. I. D. F. A. Mariz, I. S. Millichamp, J. C. De la Cal, J. R. Leiza, *Prog. Org. Coat.,* 2010, **68**, 225.
27. S. K. Dhoke, T. J. M.Sinha, P. Dutta, A. S. Khannaa, *Prog. Org. Coat.,* 2008, **62,** 183.
28. U. Konwar, N. Karak and M. Mandal, *Prog. Org. Coat.,* 2010, **68**, 265.
29. M. Behzadnasa, S. M. Mirabedini, K. Kabiri, and S. Jamali, *Corros. Sci.,* 2011, **53** 89.
30. E. Zagara and M. Zigona, *Prog. Polym Sci.,* 2011, **36**, 53.
31. R. C. S. Araujo, and V. M. D. Pasa, *Prog. Org. Coat.,* 2004, **51**, 6.
32. L. Zhang, H. K. Jeon, J. Malsam, R. Herrington and C. W. Macosko, *Polym.,* 2007, **48**, 6656.

33. P. Ferreira, R. Pereira, J. F. J. Coelho, A. F. M. Silva and M.H. Gil, *Int. J. Bio. Macro.,* 2007, **40 (2),** 144.
34. R. A. Azzam, S. K. Mohamid, R. Tol, V. Everaert, H. Reynaers, B. Goderis, *Polym. Degr. Stab.,* 2007, **92**, 480.
35. A. A. Ganash, *Polymer composite,* **2013**, DOI 10.1002/pc.22527.
36. V. P. Shinde and P. P. Patil, *J. Solid State Electrochem.* 2013, **17**, 29.
37. N. Tanveer, M. Mobin, *J. Mineral & Mat. Charact. & Eng.* 2011, **10**, 735.
38. S. Ahmad, U. Riaz, M. Kashif and M. S. Khan, *J. Inorg. Orgmet. Polym Mat.,* 2012, **22**, 662.
39. S. Ahmad, U. Riaz and J. Alam, *Adv. Polym. Tech.,* 2009, **28**, 26.
40. A. M. Mathew and P. Predeep, *Prog. Org. Coat*., 2012, **74**, 14.
41. R. J. Mortimer, *Electrochim Acta,* 1999**, 44**, 2971.
42. J. Alam, U. Riaz, S. M. Ashraf and S. Ahmad, *J. Coat. Technol. Res*., 2008, **5**, 123.
43. A. Conde, M. A. Arenas, A. De Frutos and J. De Damborenea, *Electrochim. Acta,* 2008, **53***,* 7760.
44. A. C. C. de Leon, R. B. Pernites and R. C. Advincula, *ACS Appl. Mater. Interfaces,* 2012, **4**, 3169.
45. S. K. Singh, S. P. Tambe, G. Gunasekaran, V. S. Raja and D. Kumar, *Corro. Sci*., 2009, **51**, 595.
46. O. Yavuz, M. K. Ram, M. Aldissi, P. Poddar, S. Hariharan, *J. Mater. Chem.* 2005, **15**, 810.
47. P. Sharma, D. K. Kanchan, N. Gondaliya, *Open J. Org. Polym. Mat.* 2012, **2**, 38.
48. M. T. Rodríguez, S. J. Garcia, R. Cabello, J. J. Suay and J. J. Gracenea, *J. Coat. Tech. Res*., 2005, **2**, 557.
49. S. Skale, V. Dolecek and M. Slemnik, *Prog. Org. Coat*., 2008, **62**, 387.
50. R. Naderi, M. M. Attar and M. H. Moayed, *Prog. Org. Coat*., 2004, **50**, 162.
51. M. Rohwerdera, L. M. Ducb and A. Michalika, *Electrochim. Acta.,* 2009, **54**, 6075.
52. R. S. Jadhav, D. G. Hundiwale and P .P. Mahulikar, *J. Coat. Technol. Res*., 2010, **7**, 449.
53. S. Chaudhari, P. P. Patil, A. B. Mandale, K. R. Patil, S. R. Sainkar, *J. Appl. Polym. Sci.* 2007,**106**, 220.
54. H. Wei, D. Ding, S. Wei, Z. Guo, J. Mater. Chem. A, 2013, 1, 10805.
55. T. D. Nguyen, T. A. Nguyen, M. C. Pham, B. Piro, B. Normand, H. Takenouti, *J. Electroanalyt. Chem.* 2004, **572,** 225.
56. P Li, T. C Tan, J. Y. Lee, *Synth. Metal* 1997, **88**, 237.
57. A. C. C. de Leon, R. B. Pernites, R.C. Advincula, *App. Mat. Interfaces* 2012, **4**, 3169

Fig. and captions

Table- 1 Physico-chemical and Physico-mechanical performance of COPU, 0.25POT/COPU, 0.5 POT/COPU and 1.0POT/COPU coatings.

Table- 2 Potentidynamic polarization parameter for uncoated, COPU and POT/COPU coated MS substrate in 3.5%HCl

Table- 3 Electrochemical kinetic parameters derived from EIS plots of COPU in 3.5%HCl

Table- 4 Electrochemical kinetic parameters derived from EIS plots of 0.25POT/COPU in 3.5%HCl

Table- 5 Electrochemical kinetic parameters derived from EIS plots of 0.5POT/COPU in 3.5%HCl

Table- 6 Electrochemical kinetic parameters derived from EIS plots of 1.0POT/COPU in 3.5%HCl

Fig. 1 Synthesis of COPU and POT/COPU composite

Fig. 2 FTIR spectra of POT/COPU

Fig. 3 UV-Vis Spectra of POT and different compositions of POT/COPU

Fig. 4 TEM micrographs of (a) COPU and (b) POT/COPU

Fig. 5 X-ray diffraction patterns of POT (a) and POT/COPU (b)

Fig. 6 TGA thermogram of POT, COPU and POT/COPU

Fig. 7 Plot showing the change in conductivity with increased loading of POT in COPU

Fig. 8 Corrosion rate of MS, COPU and POT/COPU in 3.5%HCl

Fig. 9 Tafel plots of uncoated, COPU and POT/COPU coated MS in 3.5%HCl

Fig. 10 E_{corr} versus Time curve in 3.5%HCl

Fig. 11 Nyquist (a) and Bode plots (b) of COPU coated MS after different interval of times in 3.5 wt% HCl solution.

Fig. 12 Nyquist impedance plots as a function of exposure time obtained in 3.5 wt% HCl solution for: 0.25POT/COPU (a); 0.50 POT/COPU (b); and 1.0 POT/COPU (c)

Fig. 13 Bode plots of (a) 0.25POT/COPU (b) 0.5POT/COPU and (c) 1.0 POT/COPU in 3.5%HCl after 24, 240 and 480 h.

Fig. 14 Equivalent circuit for coated and uncoated Mild Steel (MS)

Fig. 15 SEM micrograph of (a) POT/COPU nanocomposite (b) uncoated MS after 240 h in HCl (c) COPU coated MS after 240 h in HCl (d) 1.0-POT/COPU coated MS after 480 h in HCl (e) uncoated MS after 720 h in NaCl (f) COPU coated MS after 720 h in NaCl (g) 1.0-POT/COPU coated MS after 720 h in NaCl

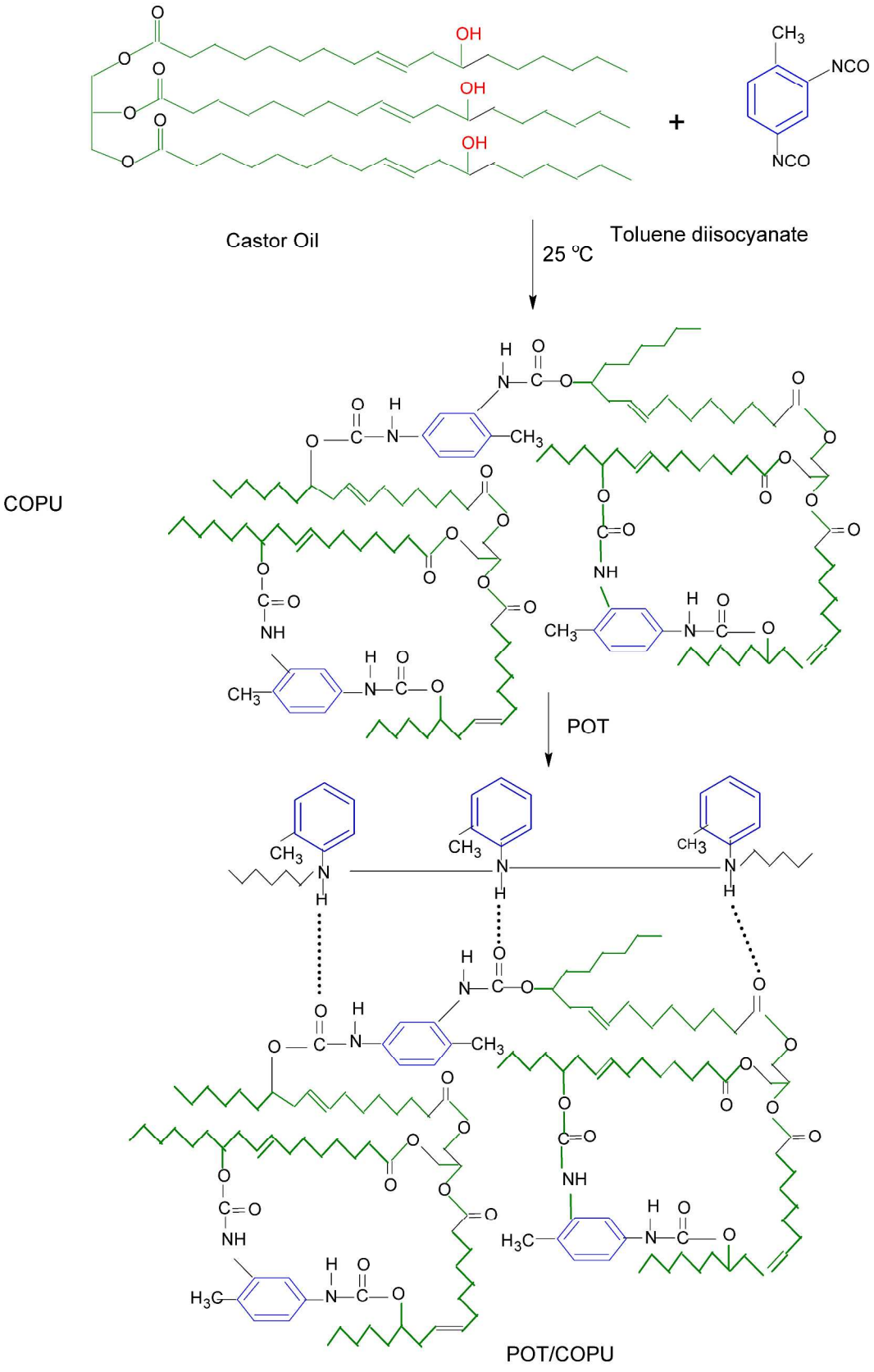

Fig. 1 Scheme for the synthesis of COPU and POT/COPU nanocomposite

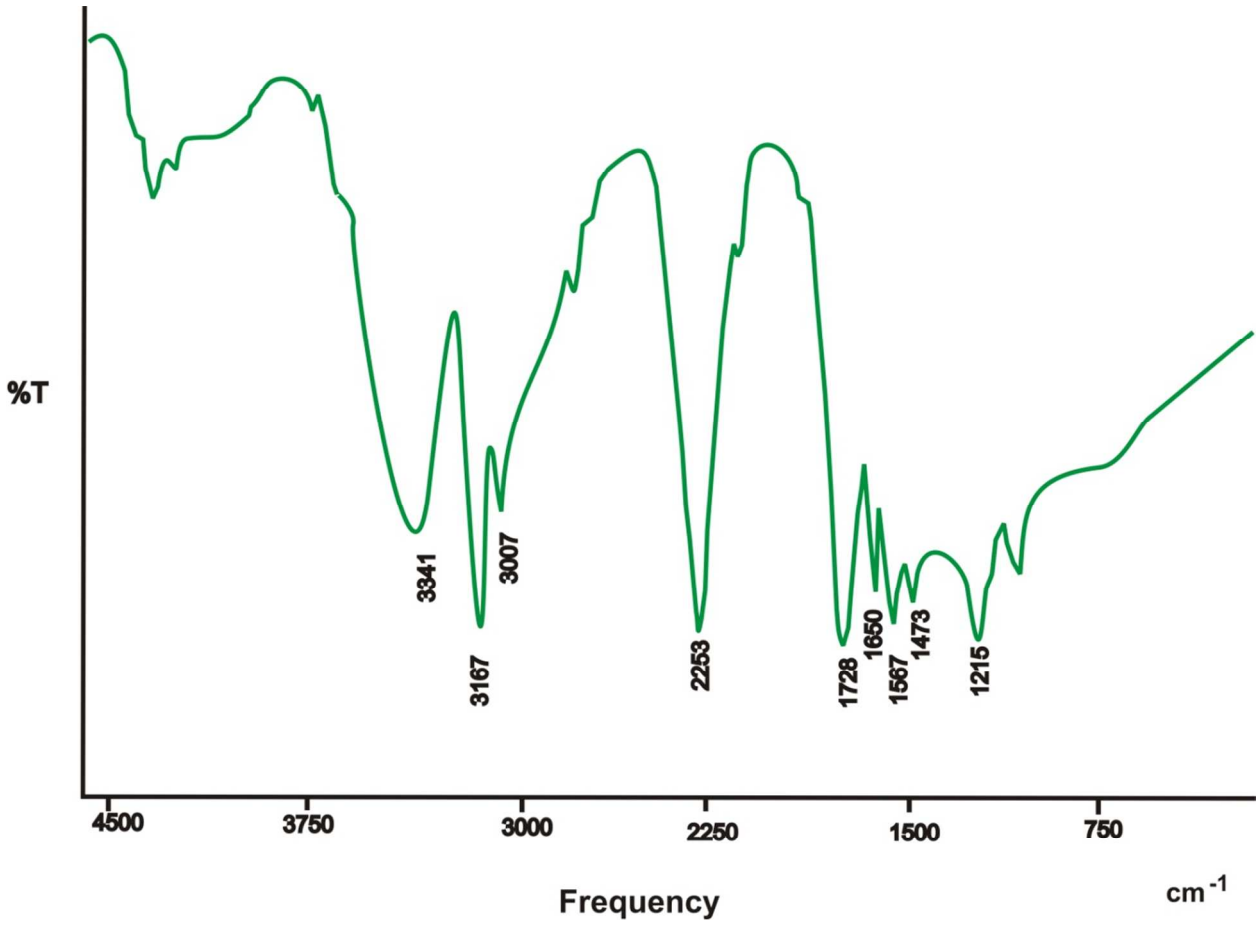

Fig. 2 FTIR spectra of POT/COPU

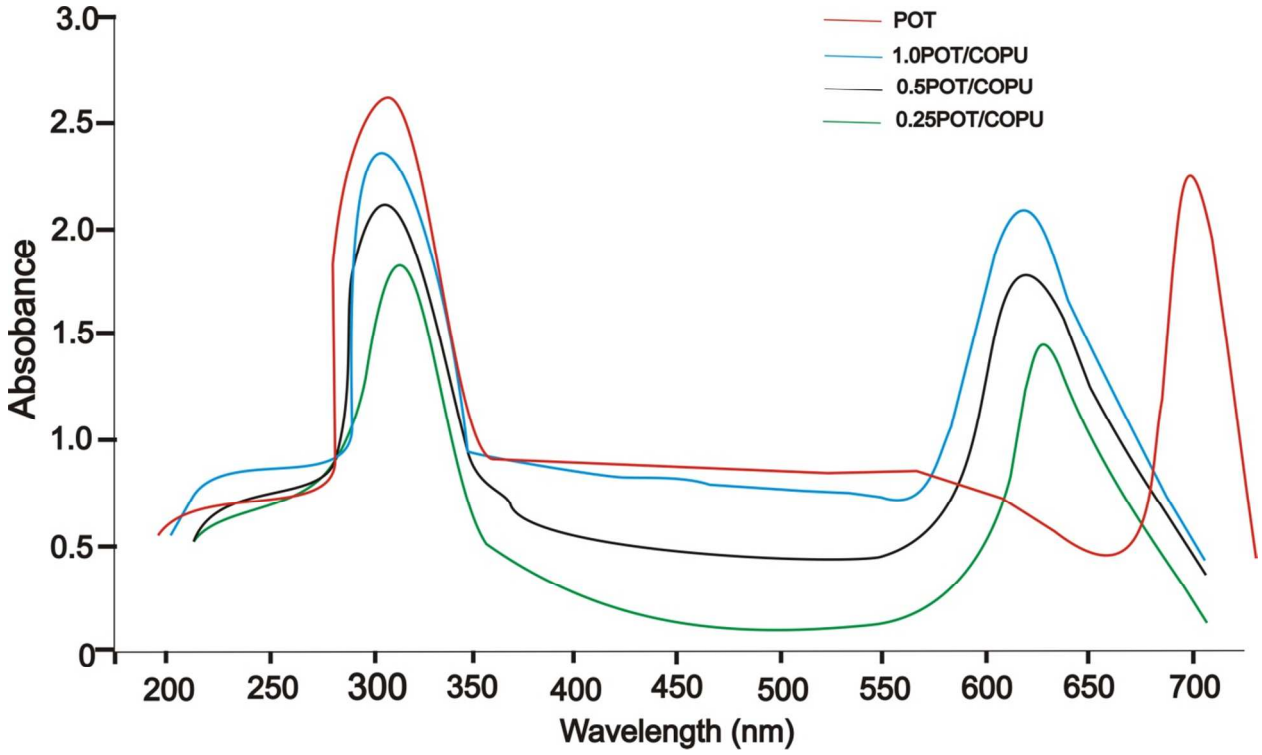

Fig. 3 UV-Vis Spectra of POT and different compositions of POT/COPU

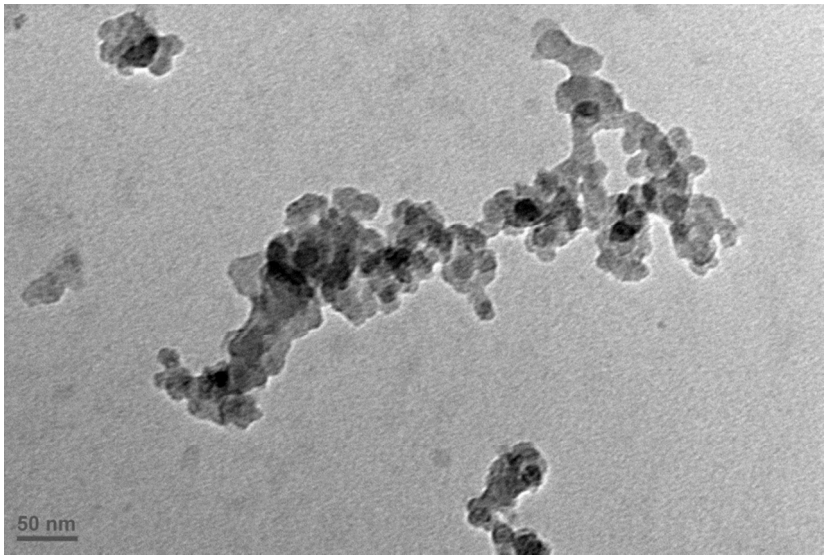

Fig. 4 TEM micrographs of POT/COPU

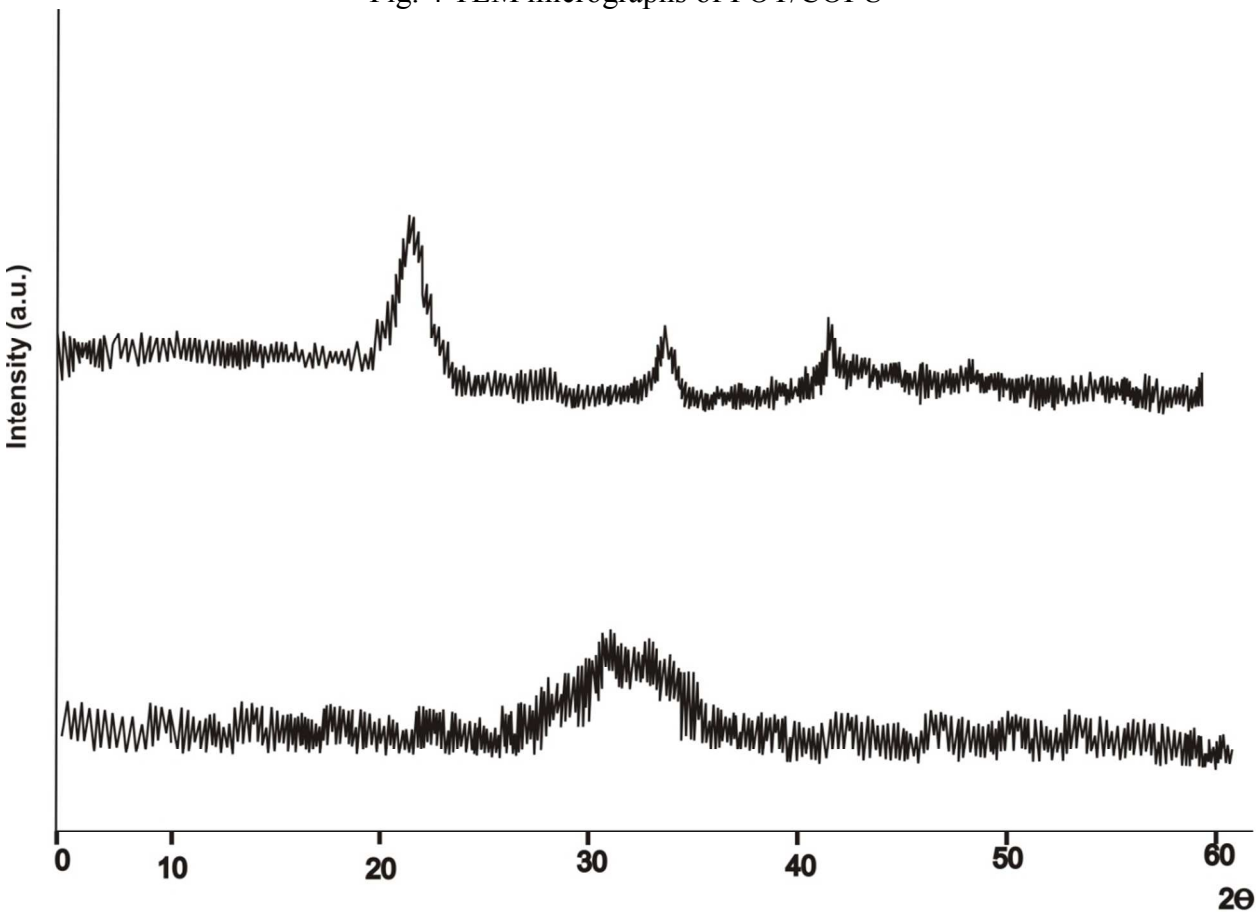

Fig. 5 X-ray diffraction patterns of POT (a) and POT/COPU (b)

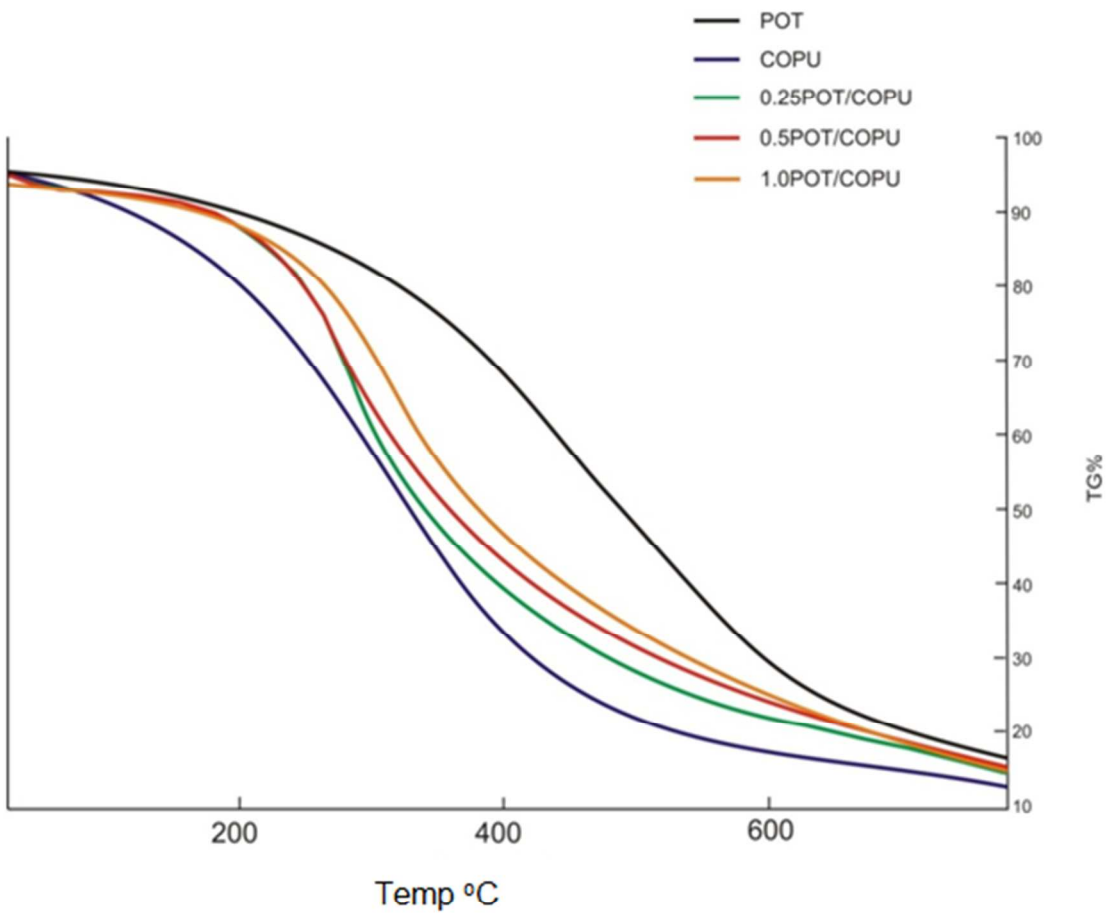

Fig. 6 TGA thermogram of POT, COPU and POT/COPU

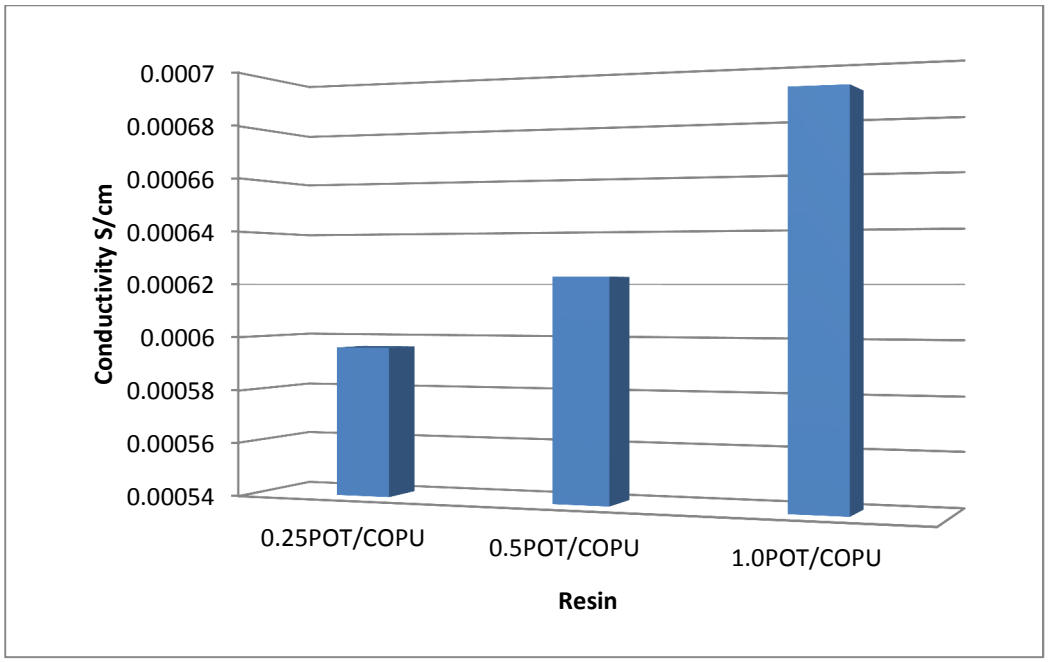

Fig. 7 Plot showing the change in conductivity with increased loading of POT in COPU

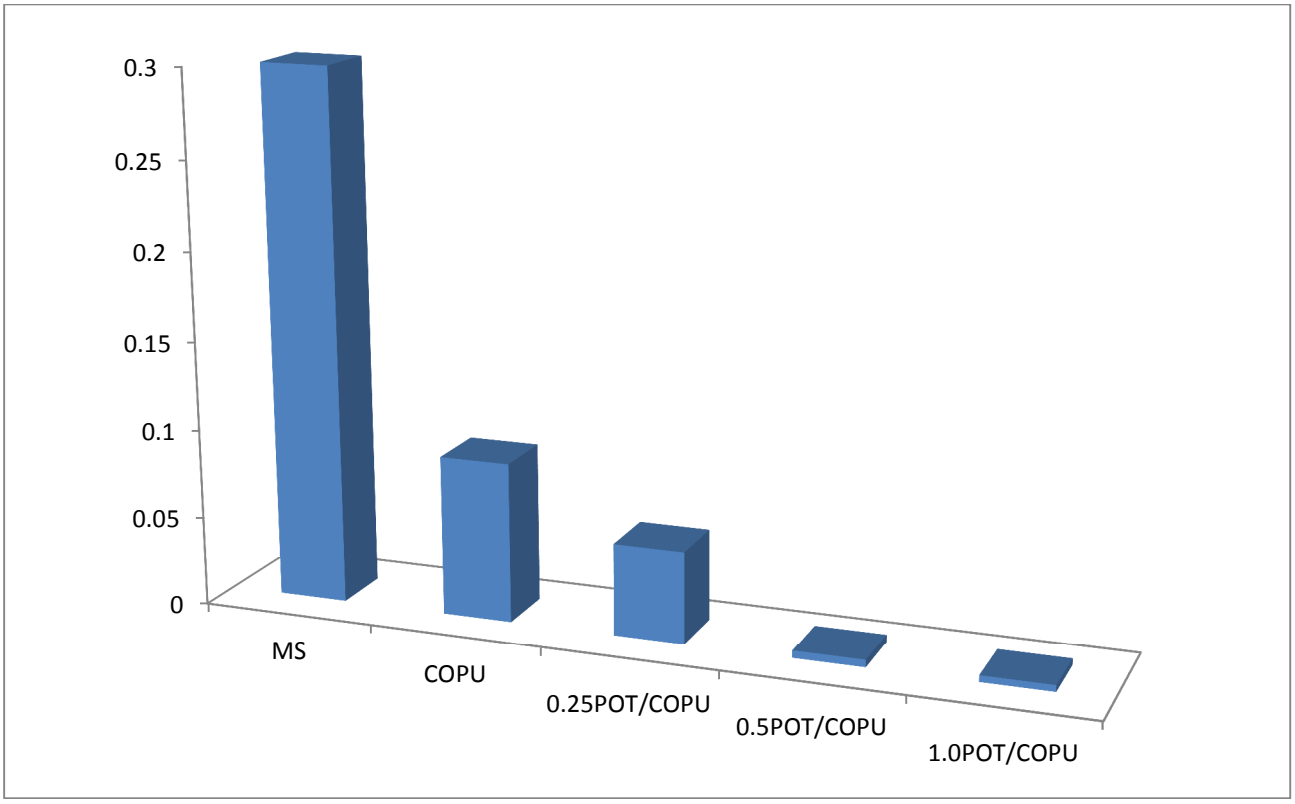

Fig. 8 Corrosion rate of MS, COPU and POT/COPU in 3.5%HCl

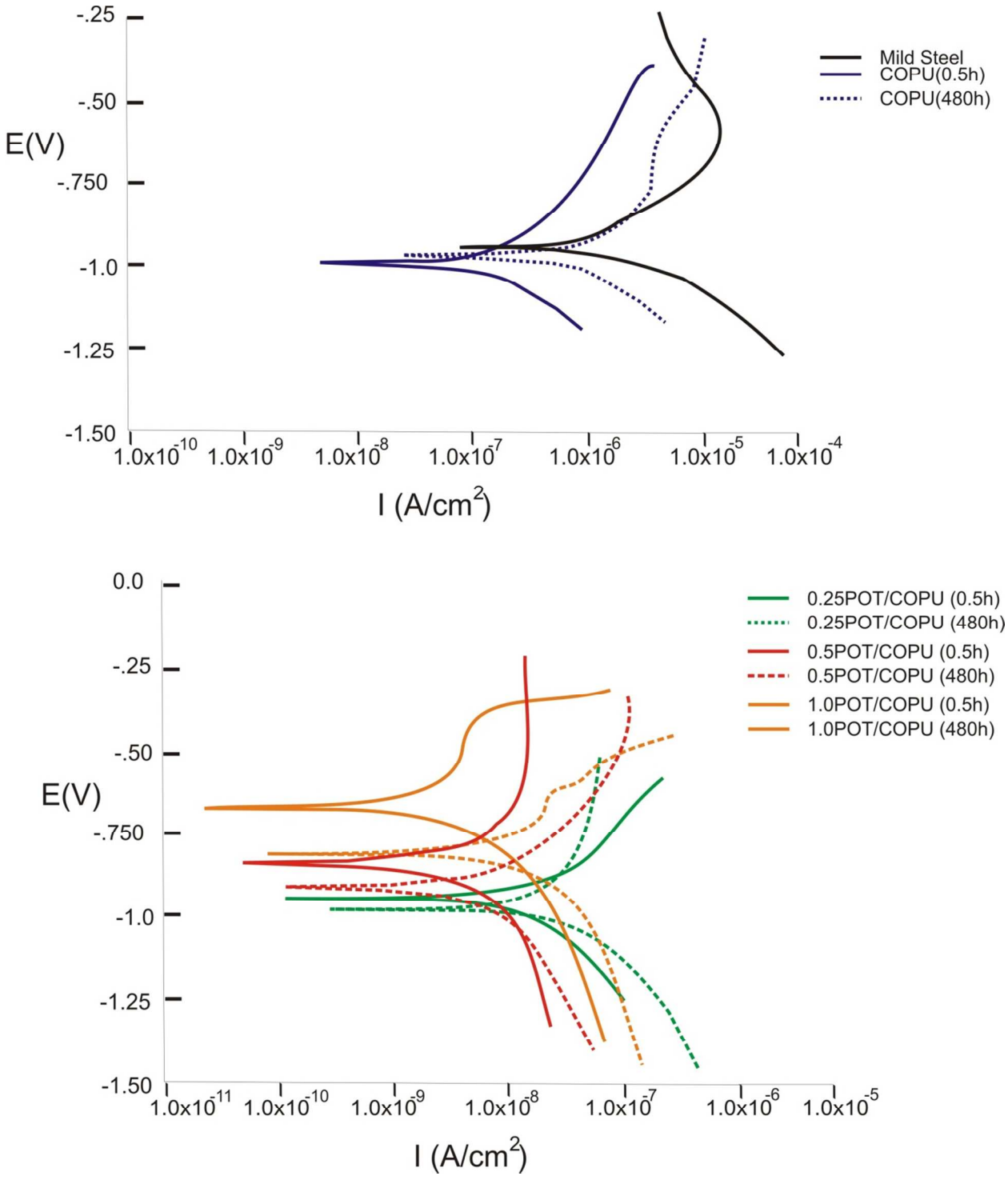

Fig. 9 Tafel plots of uncoated, COPU and POT/COPU coated MS in 3.5%HCl

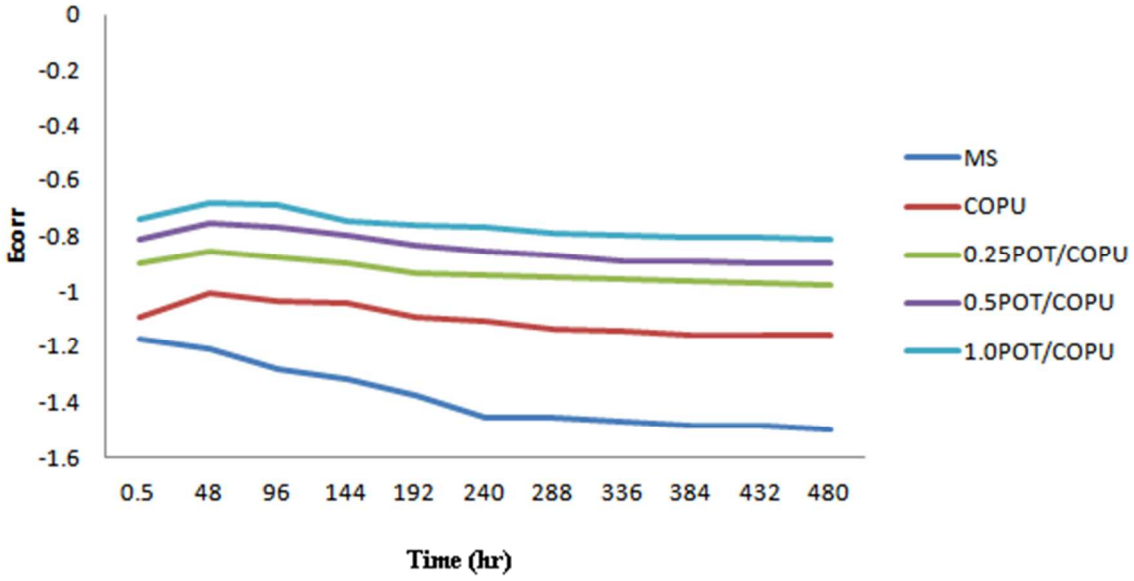

Fig. 10. E_{corr} versus Time curve in 3.5%HCl

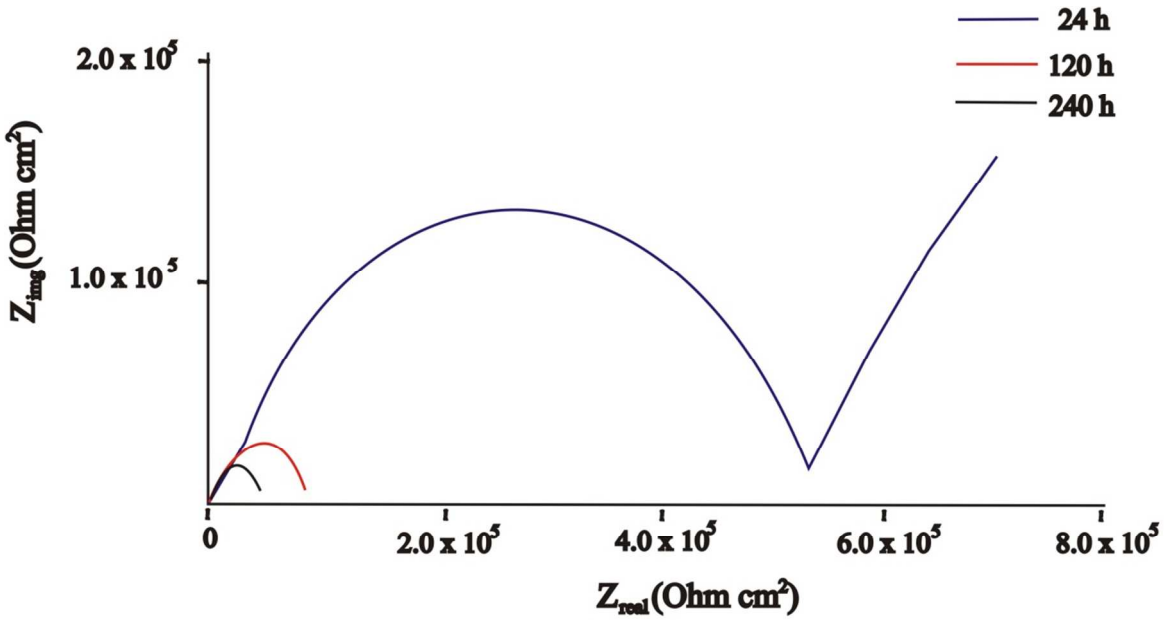

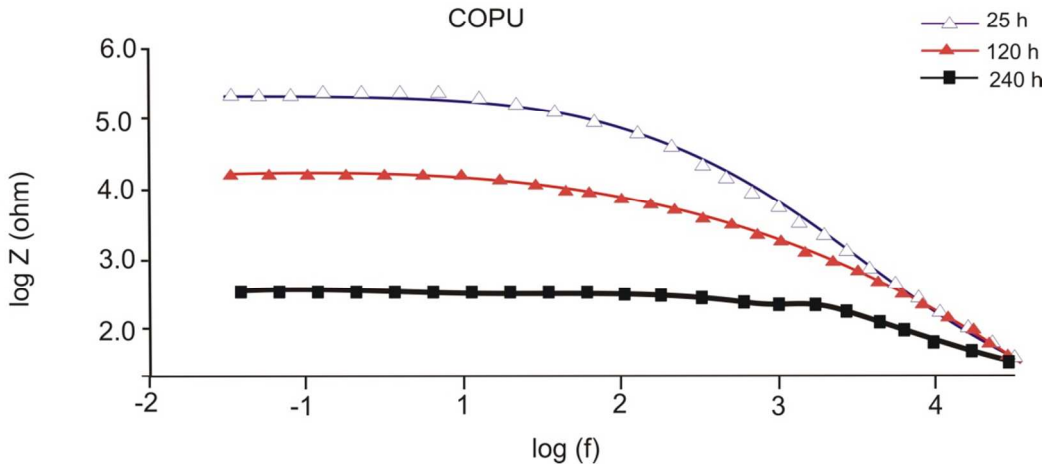

(b)

Fig. 11 Nyquist (a) and Bode plots (b) of COPU coated MS after different interval of times in 3.5 wt% HCl solution.

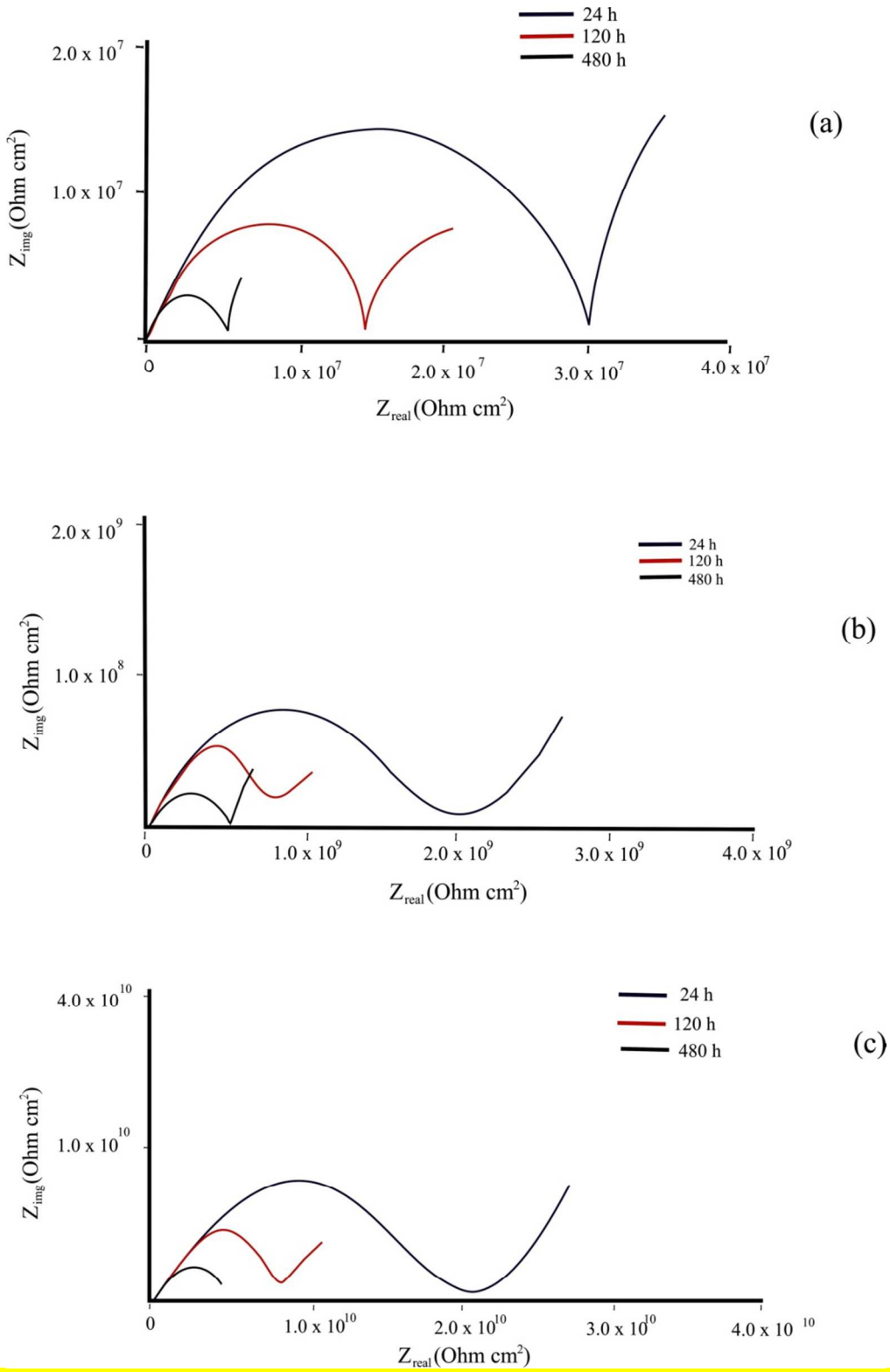

Fig. 12 Nyquist impedance plots as a function of exposure time obtained in 3.5 wt% HCl solution for: 0.25POT/COPU (a); 0.50 POT/COPU (b); and 1.0 POT/COPU (c)

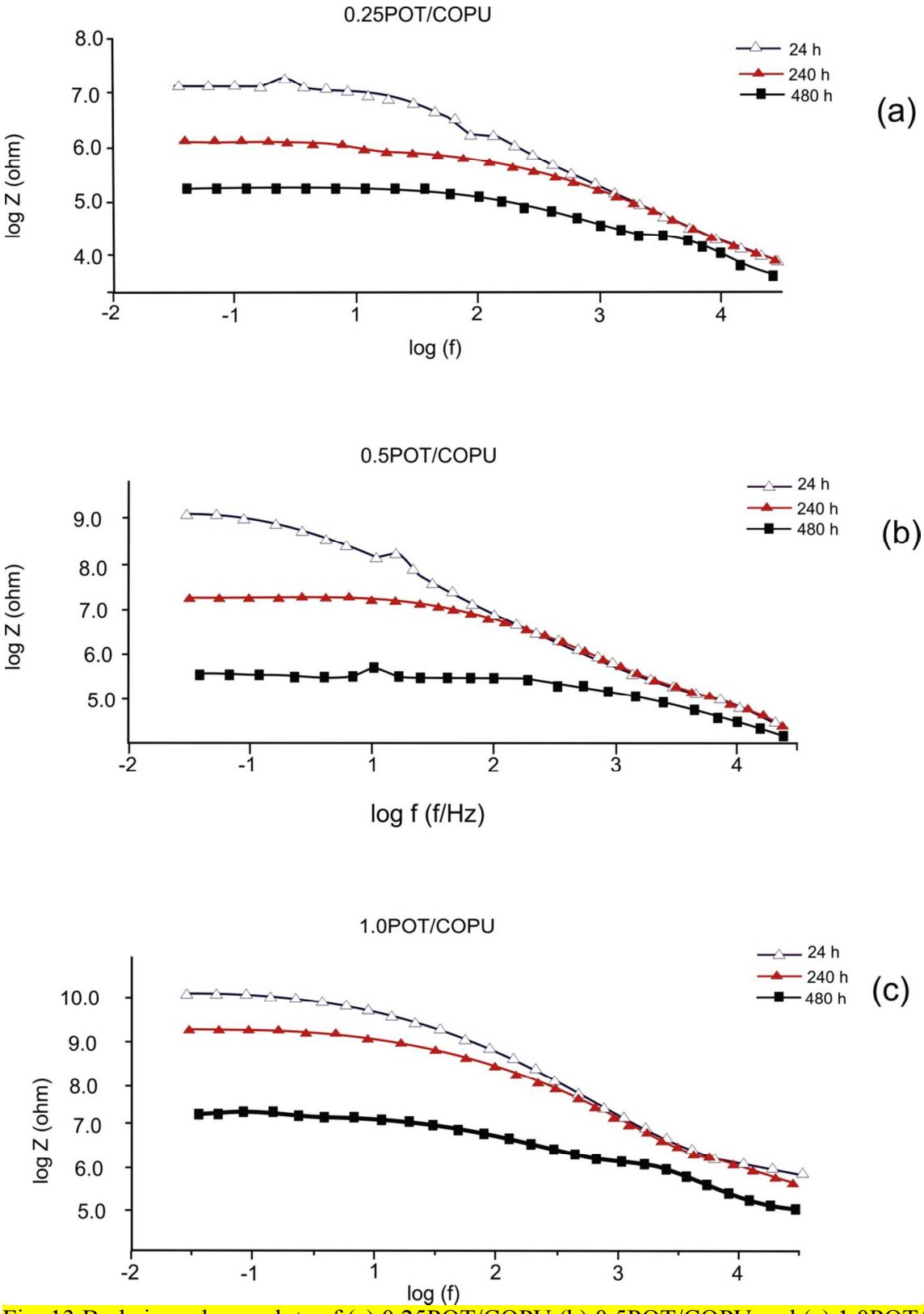

Fig. 13 Bode impedance plots of (a) 0.25POT/COPU (b) 0.5POT/COPU and (c) 1.0POT/COPU after different interval of time of exposure to 3.5 wt% NaOH solution.

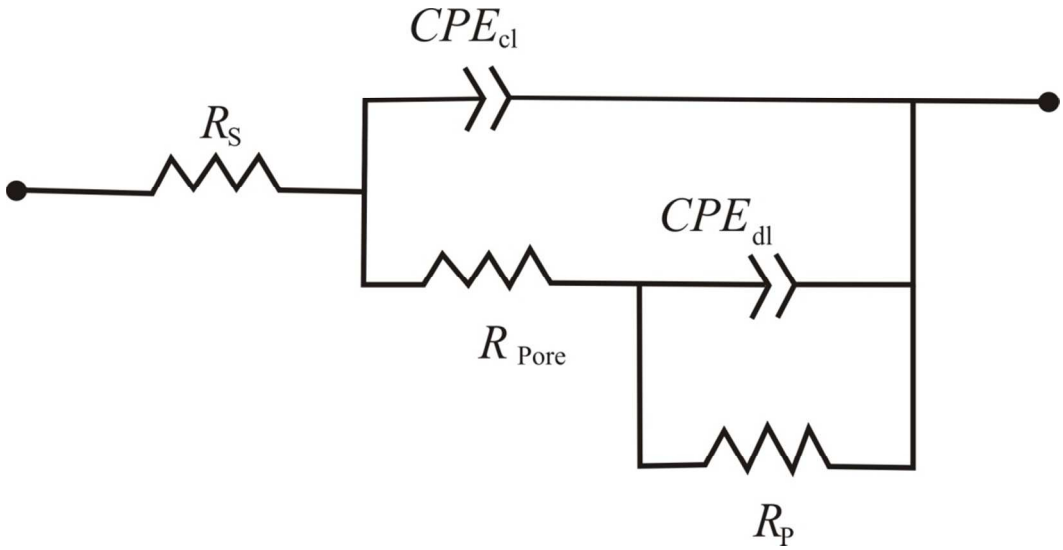

Fig. 14 Equivalent circuit for coated and uncoated Mild Steel (MS)

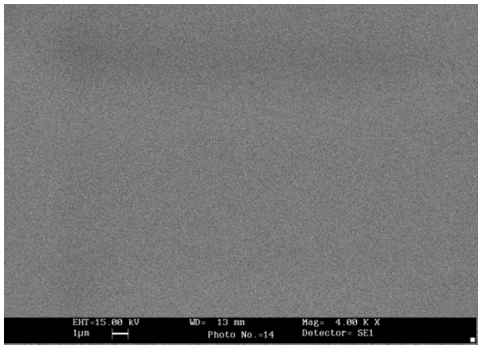

(a)

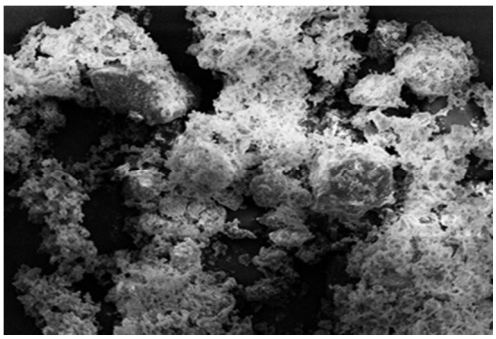

(b)

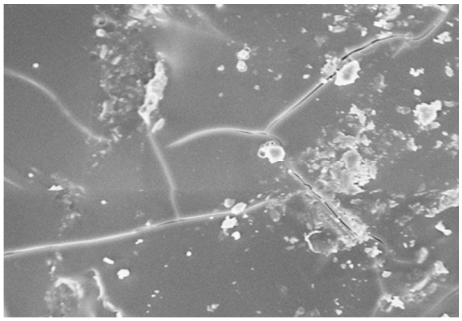

(c)

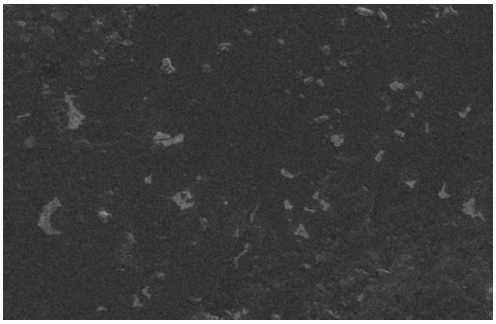

(d)

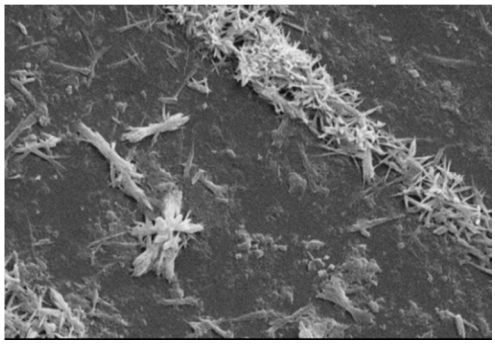

(e)

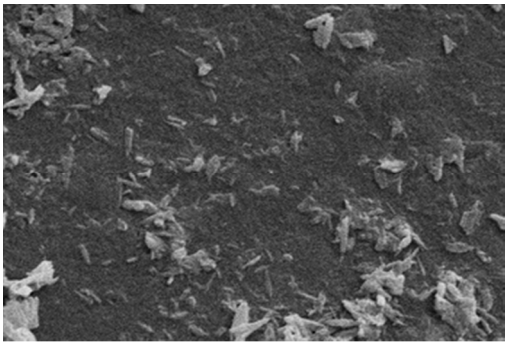

(f)

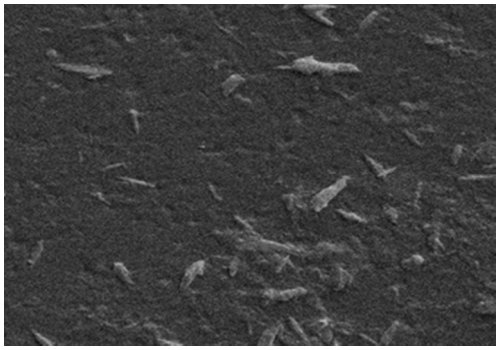

(g)

Fig. 15 SEM micrograph of (a)POT/COPU nanocomposite (b) uncoated MS after 240 h in HCl (c) COPU coated MS after 240 h in HCl (d) 1.0-POT/COPU coated MS after 480 h in HCl (e) uncoated MS after 720 h in NaCl (f) COPU coated MS after 720 h in NaCl (g) 1.0-POT/COPU coated MS after 720 h in NaCl

Table- 1. Physico-chemical and Physico-mechanical properties of COPU, 0.25POT/COPU, 0.5 POT/COPU and 1.0POT/COPU coatings.

Resin code	**COPU**	**0.25POT/COPU**	**0.5POT/COPU**	**1.0POT/COPU**
Physico-chemical Characterizations				
Specific gravity(g/ml)	1.22	1.32	1.42	1.51
Inherent Viscosity(dl/dg)	0.732	0.953	1.085	1.164
Refractive Index	1.53	1.52	1.50	1.48
Physico-mechanical Characterizations				
Gloss at 45^{o}	94	62	61	58
Scratch hardness (Kg)	1.0	7.5	7.8	8.2
Impact resistance (lb/inch)	150	200	200	200
Bending (1/8 inch)	Pass	Pass	Pass	Pass
Drying time(min)	25	15	12	10
Coating Thickness (µm)	104	104	105	104

Table- 2. Potentidynamic polarization parameter for uncoated, COPU and POT/COPU coated MS substrate in 3.5%HCl

Sample	**β-anodic (V/dec)**	**β cathodic (V/dec)**	**E_{corr}(V)**	**I_{corr} (A/cm^2)**	**IE%**
MS	0.081	0.085	-1.173	6.08x 10^{-5}	-
COPU (0.5 h)	0.137	0.114	-1.091	5.14x10^{-6}	91.44
COPU (240h)	0.139	0.161	-1.162	2.86 x10^{-5}	53.59
0.25POT/COPU (0.5h)	0.175	0.523	-0.902	9.90x10^{-8}	99.88
0.25POT/COPU (480h)	0.807	0.877	-0.978	6.48x10^{-6}	89.34
0.50POT/COPU (0.5h)	0.465	0.399	-0.812	2.92x10^{-7}	99.52
0.5POT/COPU (480h)	0.585	0.387	-0.898	9.58 x10^{-7}	96.84
1.0POT/COPU(0.5 h)	0.152	0.199	-0.738	8.30x10^{-8}	99.86
1.0POT/COPU(480 h)	0.167	0.265	-0.811	7.19 x10^{-8}	99.76

Table- 3. Electrochemical kinetic parameters derived from EIS plots of COPU in HCl medium.

Kinetics Parameters	**Immersion Period in hours**				
	24	**120**	**240**	**360**	**480**
R_p (Ωcm^2)	5.6×10^5	8.2×10^4	1.9×10^4	7.8×10^3	6.7×10^2
R_{pore} (Ωcm^2)	4.1×10^5	6.3×10^4	9.21×10^3	2.1×10^3	5.8×10^2
C_c (F/cm^2)	6.4×10^{-7}	9.3×10^{-7}	5.12×10^{-6}	4.7×10^{-5}	8.2×10^{-5}
C_{dl} (F/cm^2)	7.8×10^{-7}	8.5×10^{-7}	1.2×10^{-6}	5.7×10^{-5}	6.1×10^{-5}

Table- 4. Electrochemical kinetic parameters derived from EIS plots of 0.25POT/COPU in

Kinetics Parameters	Immersion Period in hours				
	24	120	240	360	480
R_p (Ωcm^2)	3.0×10^7	1.5×10^7	3.3×10^6	4.5×10^5	3.2×10^5
R_{pore} (Ωcm^2)	2.5×10^7	3.2×10^6	4.3×10^5	3.9×10^5	2.6×10^4
C_c (F/cm^2)	1.8×10^{-9}	4.0×10^{-9}	3.9×10^{-8}	4.5×10^{-7}	5.2×10^{-7}
C_{dl} (F/cm^2)	3.2×10^{-9}	3.5×10^{-10}	4.9×10^{-9}	3.5×10^{-9}	5.4×10^{-9}

Table- 5. Electrochemical kinetic parameters derived from EIS plots of 0.5POT/COPU in

Kinetics Parameters	Immersion Period in hours				
	24	120	240	360	480
R_p (Ωcm^2)	2.0×10^9	3.5×10^8	1.3×10^7	4.5×10^6	1.2×10^5
R_{pore} (Ωcm^2)	2.0×10^9	5.2×10^8	3.5×10^8	2.9×10^6	5.6×10^5
C_c (F/cm^2)	3.8×10^{-9}	4.5×10^{-9}	3.7×10^{-8}	2.5×10^{-7}	4.9×10^{-7}
C_{dl} (F/cm^2)	2.0×10^{-9}	2.7×10^{-10}	2.9×10^{-9}	3.2×10^{-9}	5.0×10^{-9}

Table- 6. Electrochemical kinetic parameters derived from EIS plots of 1.0POT/COPU in 3.5%HCl

Kinetics Parameters	**Immersion Period in hours**				
	24	**120**	**240**	**360**	**480**
R_{pore} **(Ωcm^2)**	3.0×10^{10}	2.5×10^{10}	2.8×10^{9}	1.5×10^{8}	5.2×10^{7}
R_p **(Ωcm^2)**	2.8×10^{10}	3.4×10^{10}	5.5×10^{9}	3.7×10^{9}	4.6×10^{7}
C_c **(F/cm^2)**	2.6×10^{-10}	3.5×10^{-9}	4.7×10^{-9}	2.8×10^{-8}	5.9×10^{-7}
C_{dl} **(F/cm^2)**	4.1×10^{-10}	5.7×10^{-9}	2.9×10^{-9}	2.2×10^{-8}	5.7×10^{-8}

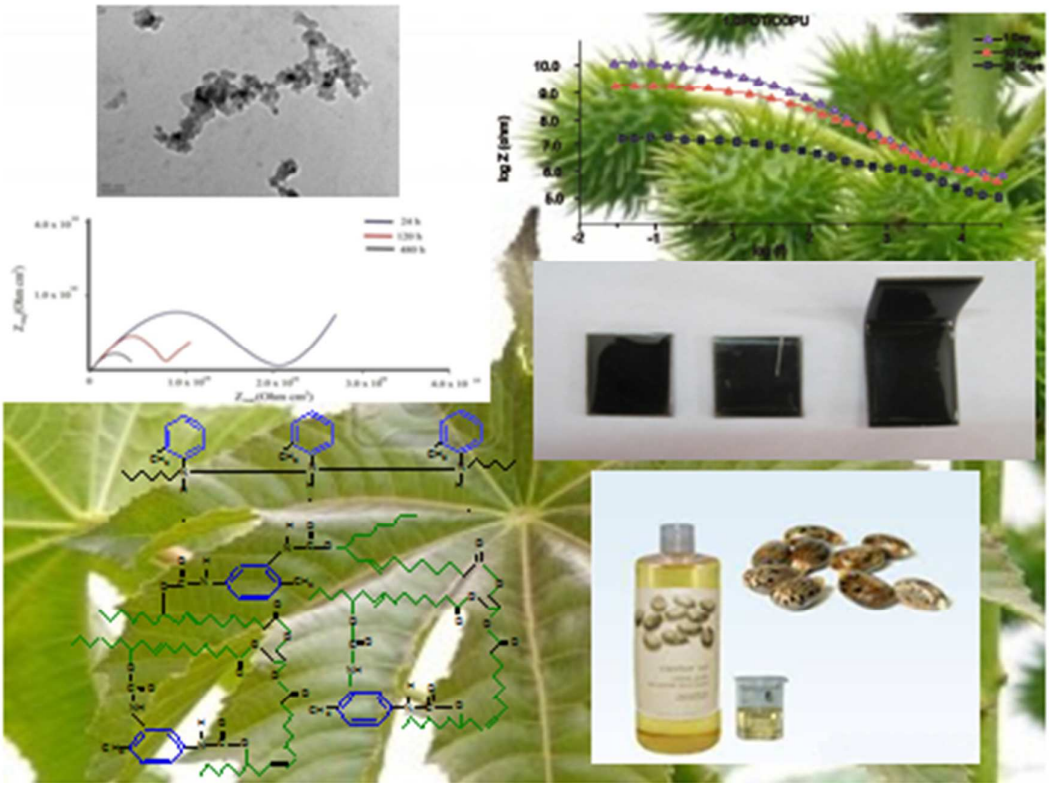

Conducting Polymer (polyorthotoluidine) dispersed castor oil polyurethane nanocomposite coatings were synthesized showing remarkably higher corrosion resistant performance in alkaline medium